Average CsI neutron density distribution from COHERENT data

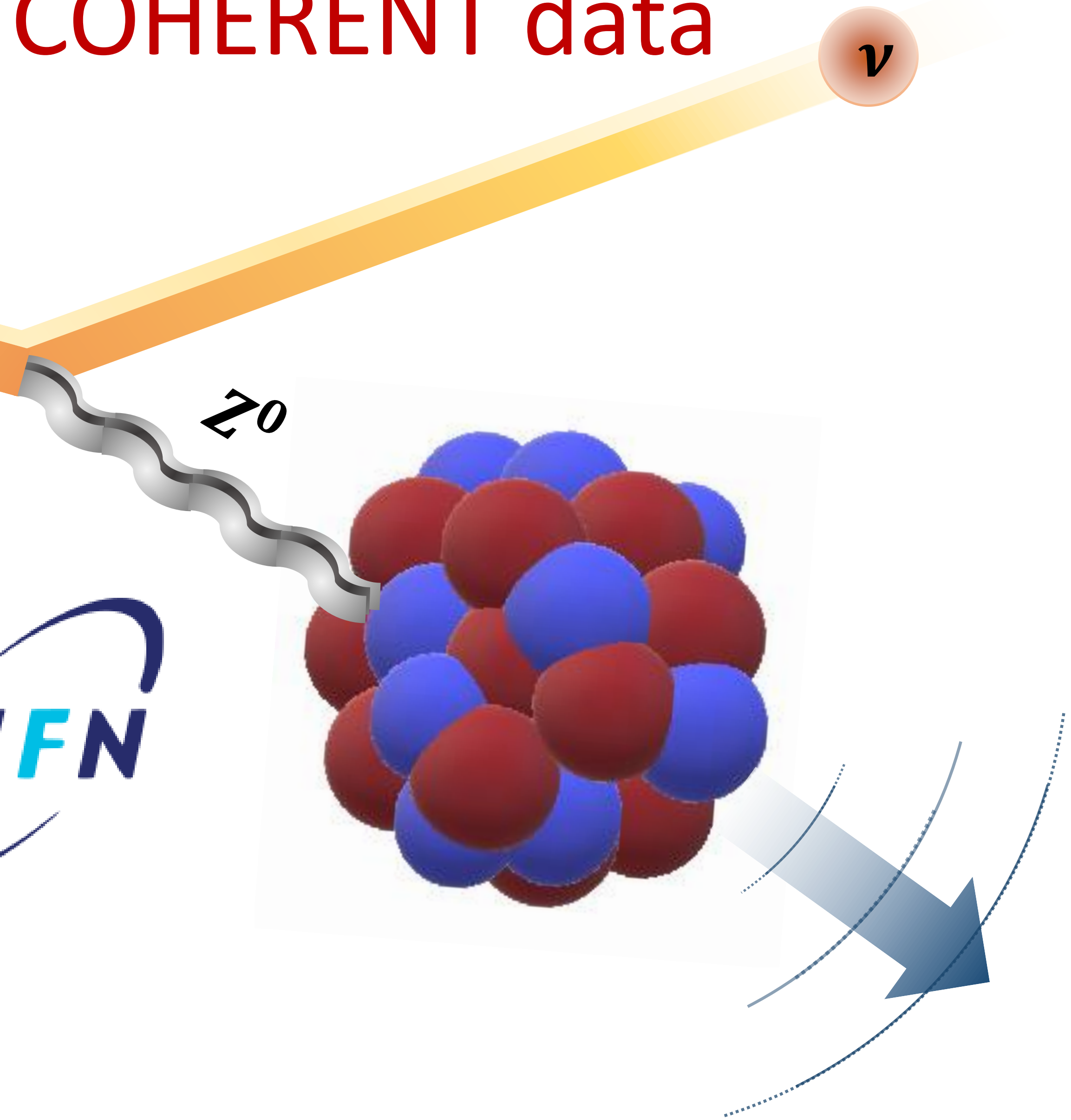

Matteo Cadeddu
INFN Cagliari

Based on M. C., C. Giunti, Y. F. Li, and Y. Y. Zhang
Phys. Rev. Lett. **120**, 072501

Summary

- Theoretical introduction to Coherent Elastic neutrino Nucleus Scattering (CEnNS)
- The role of the neutron form factor
- The COHERENT experimental result
- Tools for determination of the rms neutron distribution radius
- Results
- Conclusions and implications

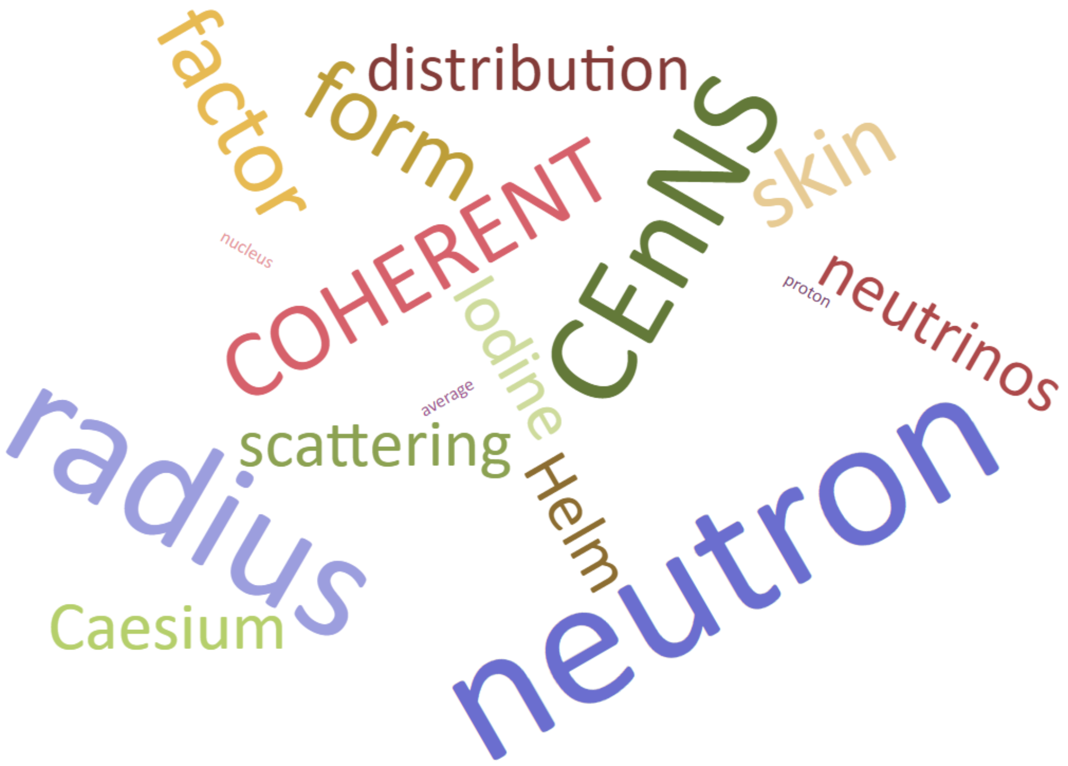

Coherent Elastic neutrino-Nucleus Scattering (CEnNS)

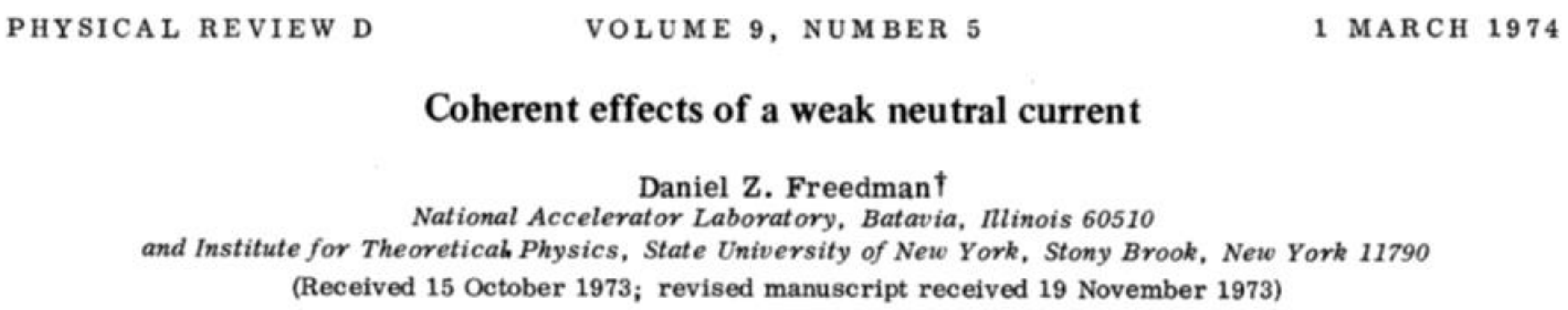
PHYSICAL REVIEW D VOLUME 9, NUMBER 5 1 MARCH 1974

Coherent effects of a weak neutral current

Daniel Z. Freedman†
National Accelerator Laboratory, Batavia, Illinois 60510
and Institute for Theoretical Physics, State University of New York, Stony Brook, New York 11790
(Received 15 October 1973; revised manuscript received 19 November 1973)

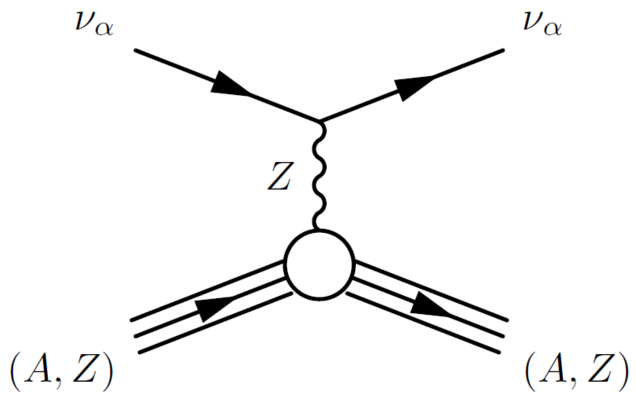

Coherent neutrino scattering on Nucleus (CNS) for a spin-zero nucleus and neglecting radiative corrections [1]

$$\boldsymbol{\nu_x + (A,Z) \rightarrow \nu_x + (A,Z)}$$

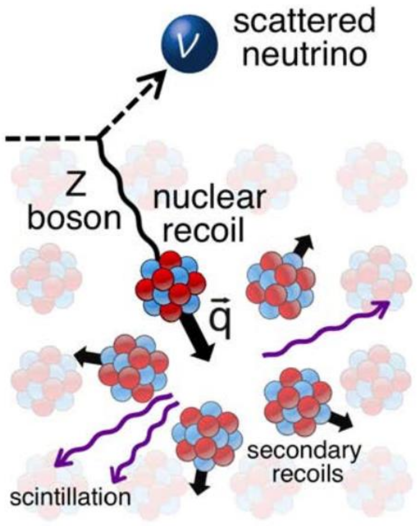

For momentum transfer small compared to inverse target size, i.e. $qR \ll 1$ ($E_\nu \lesssim 50\ MeV$)

$$\frac{d\sigma^{CEnNS}(E_\nu, E_r)}{dE_r} = \frac{G_F^2}{4\pi} Q_w^2\, m_N \left(1 - \frac{m_N E_r}{2E_\nu^2}\right) |F(E_r)|^2$$

$$\boxed{Q_w = N - \underbrace{(1 - 4\sin^2\theta_W)}_{0.0454 \pm 0.0003} Z}$$

Weak nuclear hypercharge (N number of neutrons, Z number of protons)

Unique nuclear form factor

$G_F \cong 1.16\times10^{-5}$ GeV^{-2} (Fermi constant)

θ_W (Weak mixing angle)

[1] D. Z. Freedman, Phys. Rev. D 9, 1389 (1974)

The nuclear form factor ($qR \ll 1$)

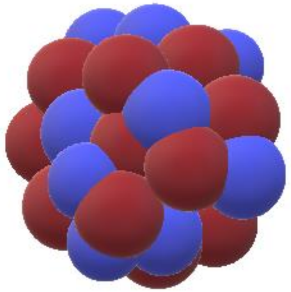

- The nuclear form factor, F(q), is taken to be the **Fourier transform** of a spherically symmetric ground state **mass distribution** normalized so that F(0) = 1:

$$F(q) = \frac{1}{M}\int \rho_{\text{mass}}(r) e^{-i\mathbf{q}\cdot\mathbf{r}} d^3r = \frac{1}{M}\int_0^\infty \rho_{\text{mass}}(r)\,\frac{\sin qr}{qr}\,4\pi r^2 dr.$$

$$\rho_{\text{mass}}(r) = \frac{m_N}{Ze}\rho_{\text{charge}}(r)$$

Assumption: Since the mass distribution in the nucleus is difficult to probe, it is generally assumed that mass and charge densities are proportional so that charge densities, determined through **elastic electron scattering** or **muonic spectroscopy data** [2] can be utilized instead.

It is convenient to have an analytic expression. This expression has been provided by the **Helm form factor** [3]

$$\boxed{F_N^{\text{Helm}}(q^2) = 3\,\frac{j_1(qR_0)}{qR_0}\,e^{-q^2s^2/2}}$$

Where j_1 is the spherical Bessel function of the first kind and $\boldsymbol{R_0}$ **is the box (or diffraction) radius,** s is the *surface thickness* and q is the **momentum transfer.** The parameters R_0 and s are usually chosen to match numerical integration of **Two-Parameter Fermi model** or other parametric models of nuclear density. For example, Lewin and Smith [4] demonstrated a method for fitting parameters in the Helm form factor to **muonic spectroscopy** data in the Fricke et al. compilation [2]

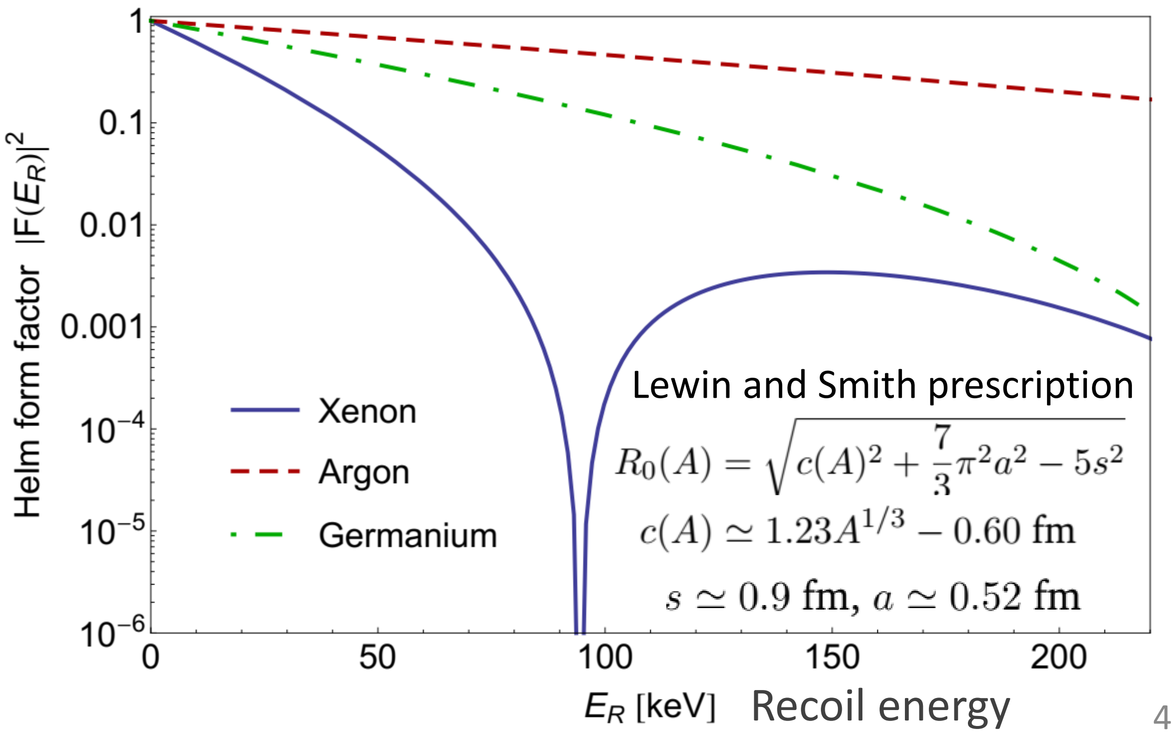

[2] G. Fricke et al. *Atom. Data Nucl. Data Tabl.* 60 (1995), pp. 177–285

[3] Helm R. *Phys. Rev.* **104**, 1466 (1956)

[4] J. D. Lewin and P. F. Smith. *Astropart. Phys.* 6 (1996), pp. 87–112

CEnNS cross sections

Typical values of the total **coherent neutrino-nucleus scattering** cross section is in the range of **$\sim 10^{-38}$ cm^2** which is at least an order of magnitude larger than other neutrino interactions in this energy range.

For example, **charged current inverse β decay on protons** has a total cross section of $\sigma_{\overline{\nu}_e p} \cong 10^{-40}$ cm^2 and **elastic neutrino-electron scattering** has a total cross section of $\sigma_{\nu_e e} \cong 10^{-43}$ cm^2 .

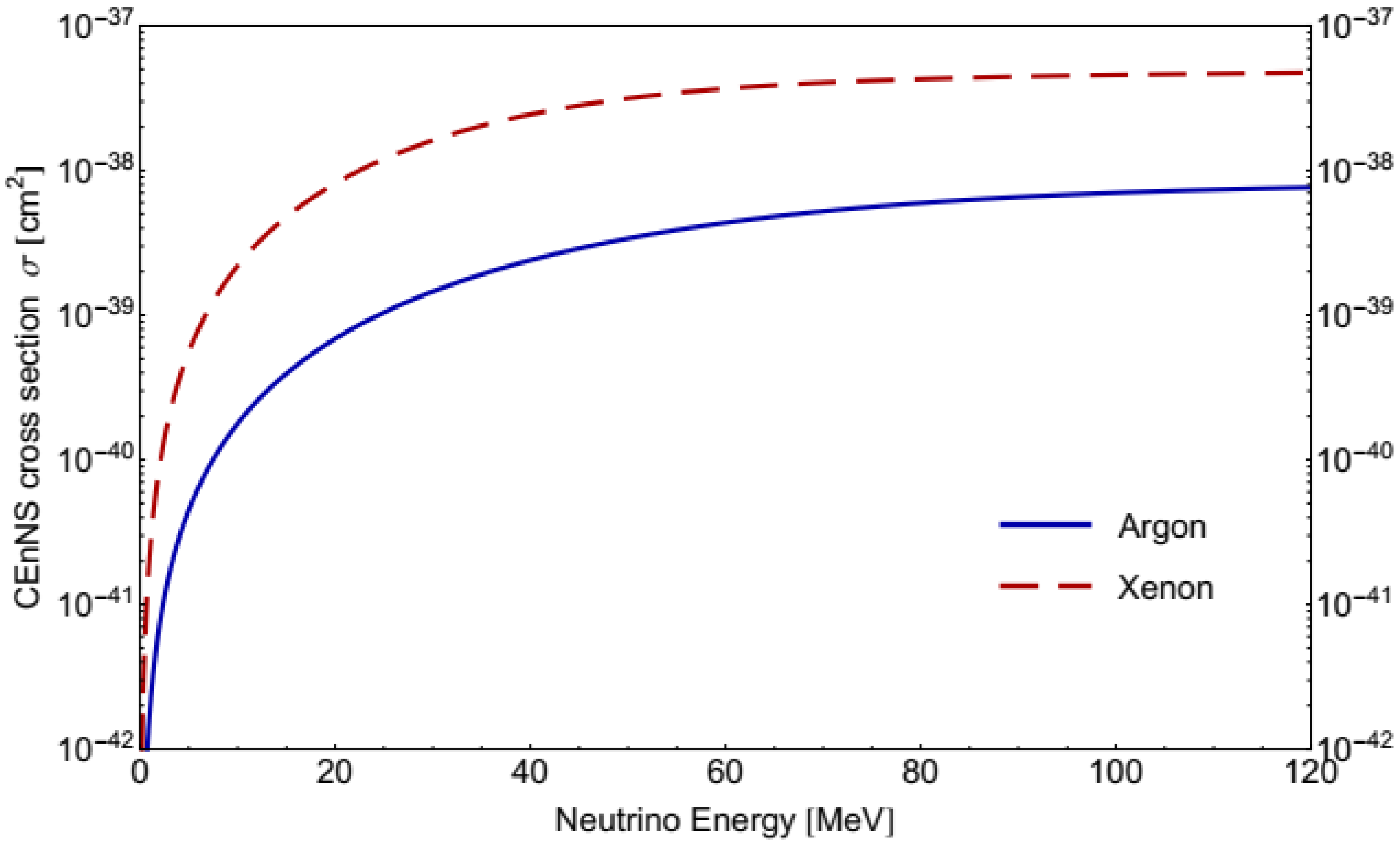

But very small recoil energy…

The maximum nuclear recoil energy for a target nucleus of mass m_N is given by $\boldsymbol{E_r^{max} = \frac{2E_\nu^2}{m_N + 2E_\nu}}$ which is in the **keV** range for $E_\nu \sim 50$ MeV. (For caesium nuclei $E_r^{max} \approx 40$ keV)

The COHERENT experiment

August 2017: First observation of CEnNS after 40 year from its prediction!

The CEnNS has eluded detection for **four decades**, even though its predicted cross-section is the largest by far of all low-energy neutrino couplings.

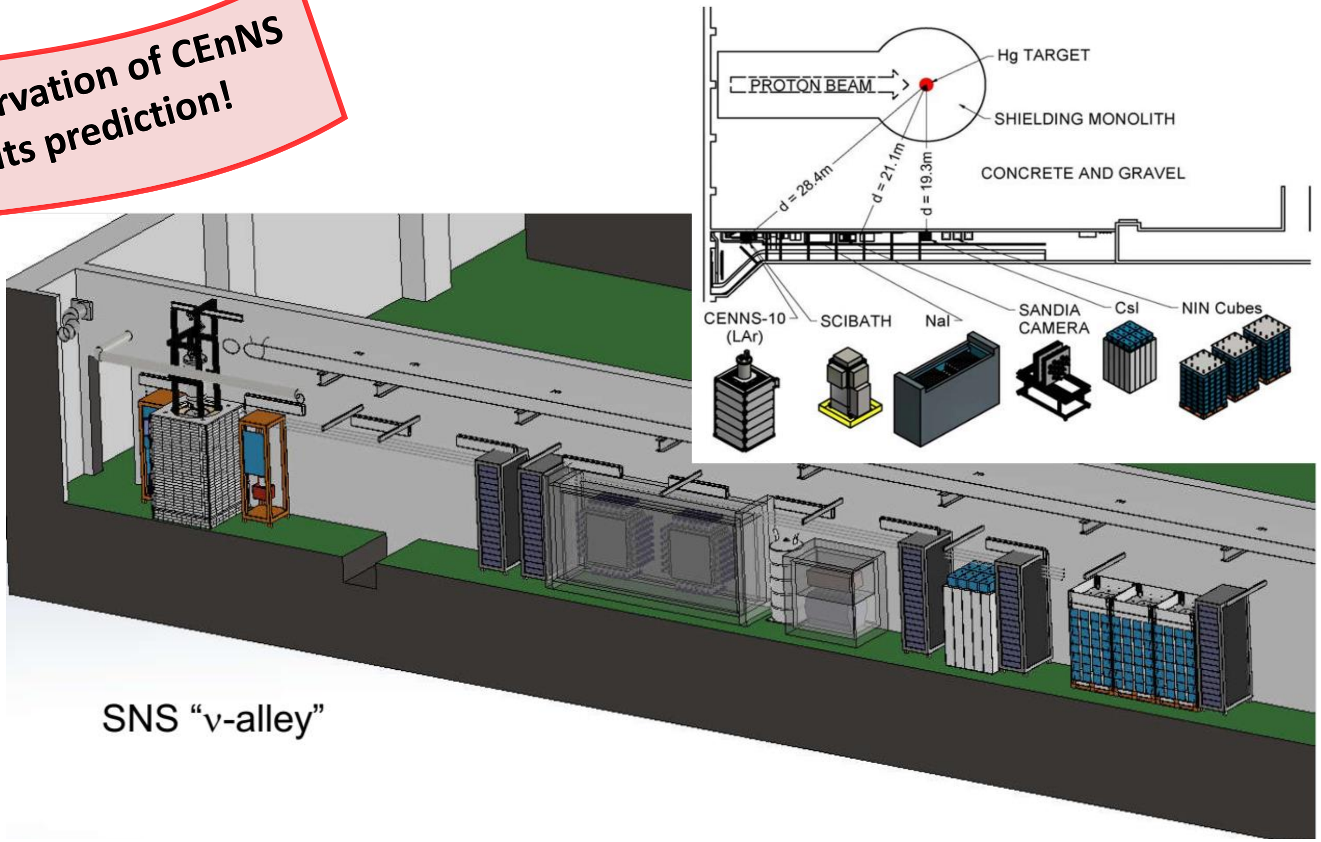

SNS “ν-alley”

*[5] D. Akimov et al. “Observation of Coherent Elastic Neutrino-Nucleus Scattering” **Science** 357.6356 (2017)*

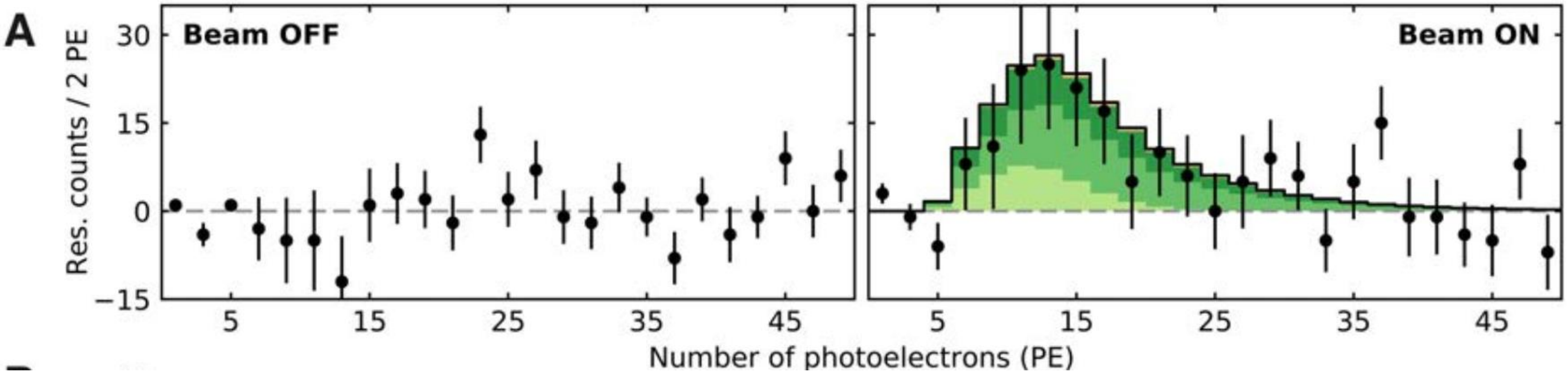

They observed this process at a 6.7σ CL, using a low-background, 14.6-kg CsI scintillator exposed to the neutrino emissions from the Spallation Neutron Source at Oak Ridge National Laboratory.

The COHERENT experiment (result)

- The Likelihood analysis [5], using the standard CEnNS cross section (**with a unique nuclear form factor**) showed that the best-fit value is **134 ± 22 CEnNS** events.

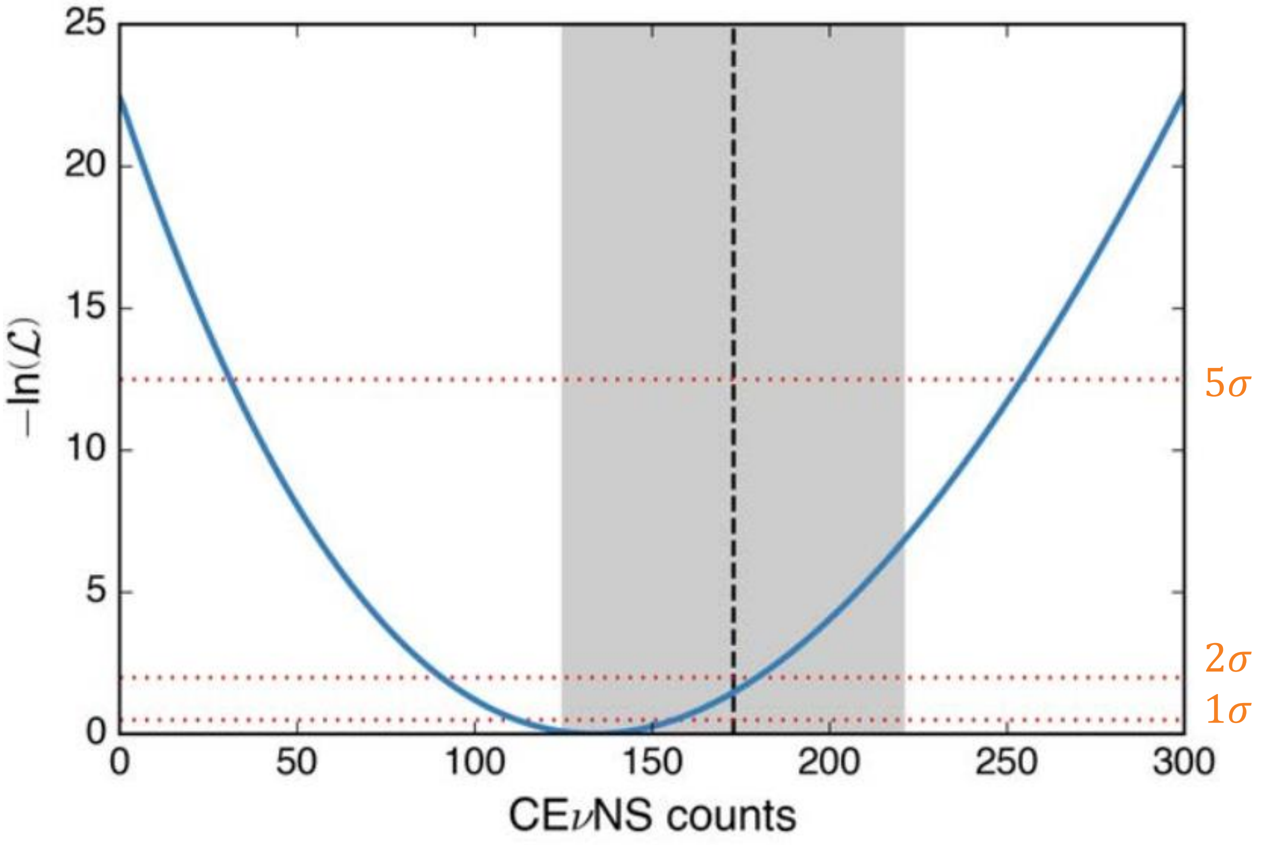

The result is within the 68% confidence band of the Standard Model prediction of **173 events**, shown as a shaded region and a vertical dashed line.

Comparison of log-likelihood values at counts of 0 and 134 indicates that the null hypothesis, corresponding to an absence of CEnNS events, is rejected at a level of 6.7-sigma, relative to the best fit.

This small discrepancy could be used to put constraints to exotic neutrino physics like **non standard interactions** between neutrinos and quarks (*arXiv: 1806.07424, PRD 97 0330033,* JHEP 1807 037, JHEP 1805 066, *PLB 775 54-57…)* *however only **relaxing the approximation of a unique form factor** for protons and neutrons it is possible to achieve a very good fit to the data.*

The CEnNS process as unique probe of the neutron density distribution of nuclei

The CEnNS process itself can be used to provide the first **model independent measurement of the neutron distribution radius**, which is basically unknown for most of the nuclei.

Even if it sounds strange, spatial distribution of neutrons inside nuclei is basically unknown!

The rms neutron distribution radius Rn and the difference between Rn and the rms radius Rp of the proton distribution (the so-called "**neutron skin**")

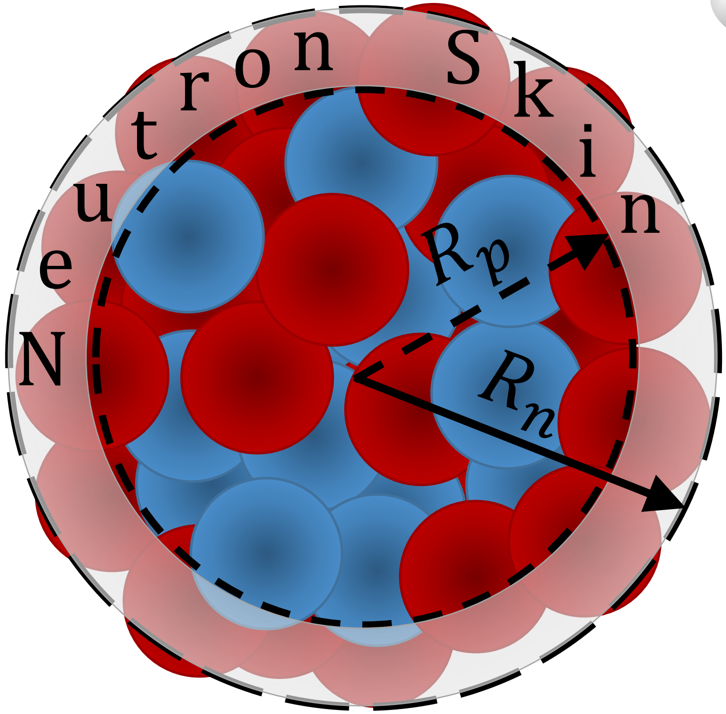

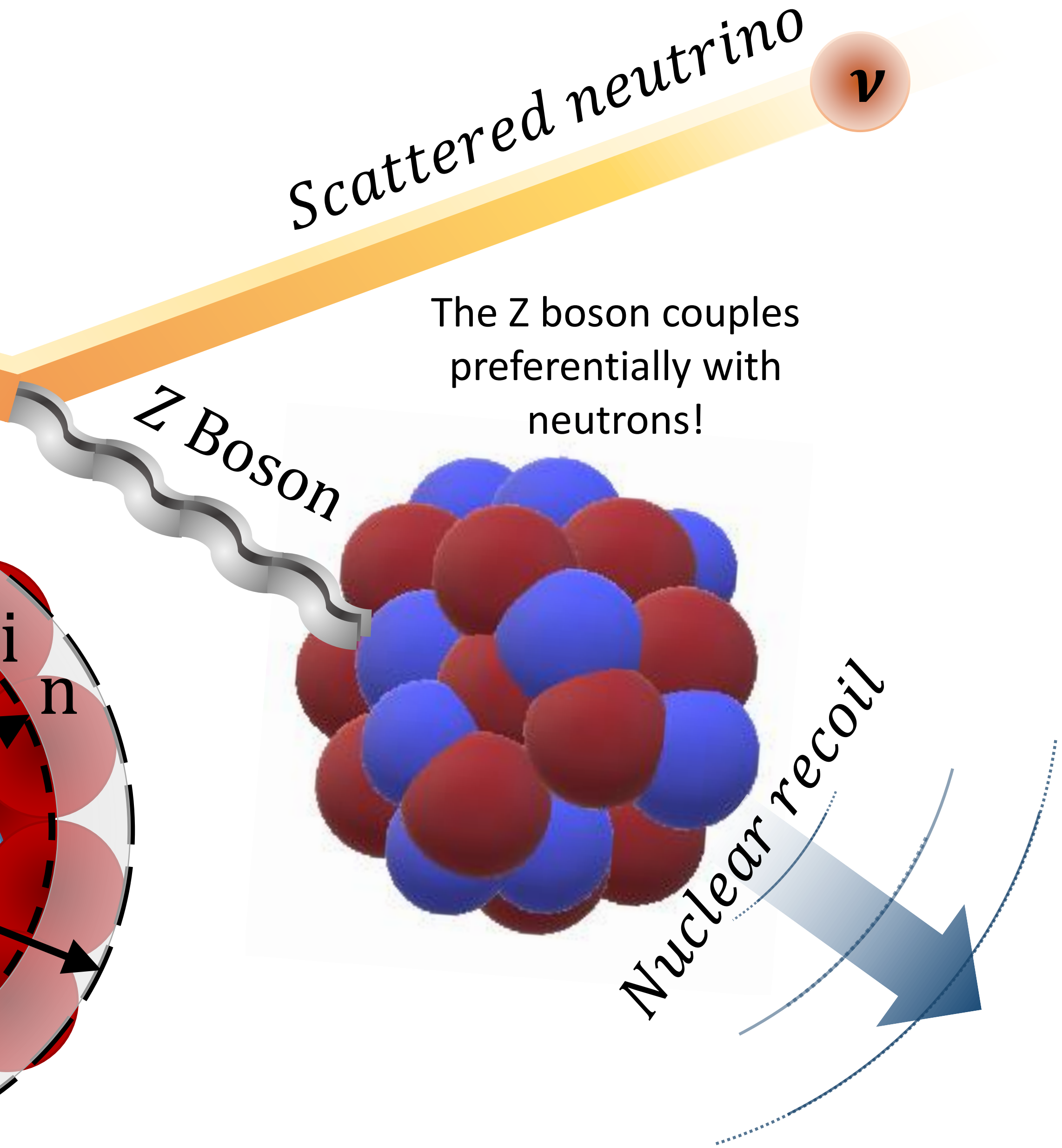

CEnNS cross section with different neutron and proton form factors

$$\frac{d\sigma_{\nu-CsI}}{dE_r} = \frac{G_F^2\, m_N}{4\pi}\left(1 - \frac{m_N E_r}{2E_\nu^2}\right)\left[N - \left(1 - 4\sin^2\theta_W\right) Z\right]^2 \boldsymbol{F_{Nucl}^2(E_r, R_{Nucl})}$$

[6] A. Drukier and L. Stodolsky, Phys. Rev. **D30**, 2295(1984).
[7] J. Barranco, O. G. Miranda, and T. I. Rashba, JHEP **0512**, 021 (2005), hep-ph/0508299.
[8] K. Patton, J. Engel, G. C. McLaughlin, and N. Schunck, Phys. Rev. **C86**, 024612 (2012), arXiv:1207.0693 [nuclth]

Two different form factors, one for the proton distribution and one for the neutron distribution

$$\frac{d\sigma_{\nu-CsI}}{dE_r} = \frac{G_F^2\, m_N}{4\pi}\left(1 - \frac{m_N E_r}{2E_\nu^2}\right)\left[N\, \boldsymbol{F_N(E_r, R_n)} - \underbrace{\left(1 - 4\sin^2\theta_W\right)} Z\, F_Z\left(E_r, R_p\right)\right]^2$$

This factor is small ~0.0454 and moreover Z<N so the contribution of the proton form factor is negligible!!

Hence, **measurements of the process give information on the nuclear neutron form factor**, which is more difficult to obtain than the information on the proton one, that can be obtained with elastic electron-nucleus scattering and other electromagnetic processes.

The proton form factor

$$\frac{d\sigma_{\nu-CsI}}{dE_r} = \frac{G_F^2\, m_N}{4\pi}\left(1-\frac{m_N E_r}{2E_\nu^2}\right)\left[N\, F_N(E_r, R_n) - (1-4\sin^2\theta_W)\; Z\, F_Z(E_r, R_p)\right]^2$$

Electron scattering and muonic spectroscopy can probes only the proton distribution

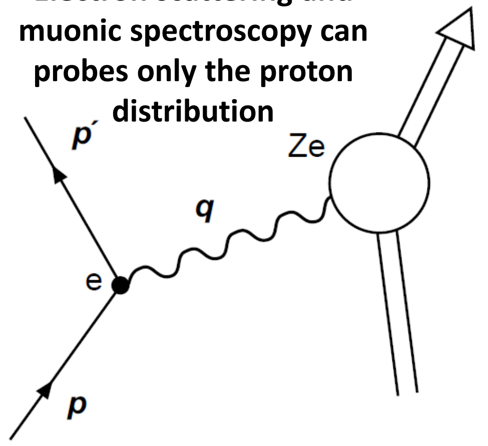

The proton structures of ${}^{133}_{55}Cs$ $(N = 78)$ and ${}^{127}_{53}I$ $(N = 74)$ have been studied with muonic spectroscopy and the data were fitted with **two-parameter Fermi density distributions** of the form

$$\rho_F(r) = \frac{\rho_0}{1+e^{(r-c)/a}}$$

Where, the half-density radius c is related to the **rms radius** and the a parameter quantifies the surface thickness **t=4aln(3)** (in the analysis fixed to 2.30 fm).

- Fitting the data they obtained

$R_p^{Cs} = 4.804$ fm (Caesium proton rms radius)

$R_p^{I} = 4.749$ fm (Iodine proton rms radius)

[9] G. Fricke et al., Atom. Data Nucl. Data Tabl. **60**, 177 (1995).

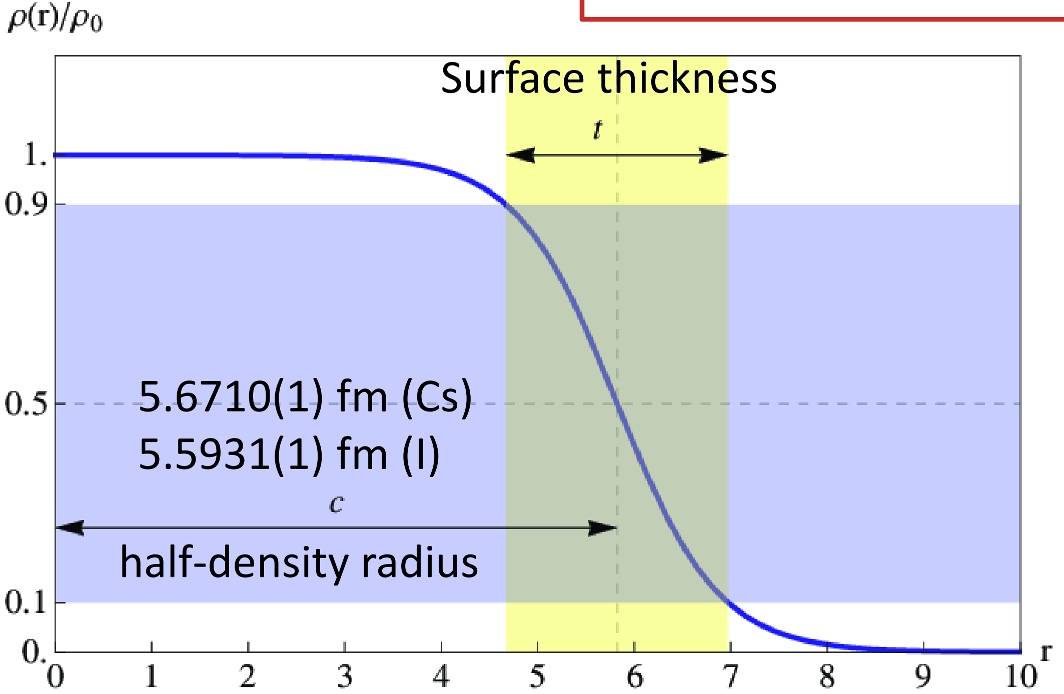

Neutron form factor parametrization

Since **it is expected that also the neutron structures of Cs and I are similar** and the current uncertainties of the COHERENT data do not allow to distinguish between them, we consider

$$F_{N,\mathrm{Cs}}(q^2) \simeq F_{N,\mathrm{I}}(q^2) \simeq F_N(q^2)$$

In order to get information on the neutron distribution of the $^{133}_{55}Cs$ and $^{127}_{53}I$ system, we considered the following parameterizations of the neutron form factor

1. **Symmetrized two-parameter Fermi form factor**

Neutron rms radius

$$R_n^2 = \frac{3}{5}c^2 + \frac{7}{5}(\pi a)^2.$$

We consider the same value of t = 2.30 fm as for the proton form factor.

2. **Helm form factor**

Neutron rms radius

$$R_n^2 = \frac{3}{5}R_0^2 + 3s^2$$

s is the surface thickness. We consider the value *s* = 0.9 fm which was determined for the proton form factor of similar nuclei.

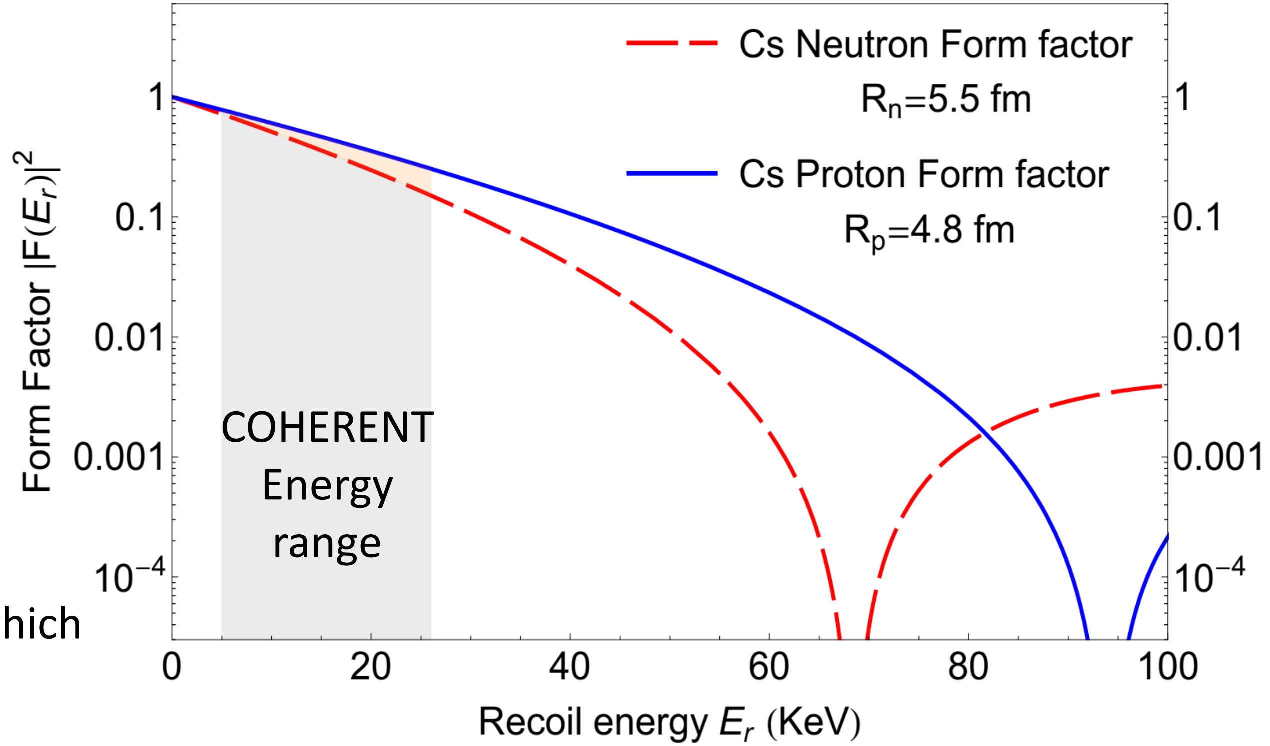

Fitting the COHERENT data: the CEnNS xsec

The theoretical number of CEnNS events in each energy bin *i* **depends on the neutron form factor** and it is given by

$$N_i^{th} = N_{CsI} \int_{E_{r\,i}}^{E_{r\,i+1}} dE_r \int_{E_{min}} dE_\nu \boxed{A(E_r)} \boxed{\frac{dN_\nu}{dE_\nu}} \boxed{\frac{d\sigma_{\nu-CsI}}{dE_r}}$$

$$E_\nu^{\min} = \frac{1}{2}\left(E_r + \sqrt{E_r(E_r + 2m_N)}\right) \simeq \sqrt{\frac{m_N E_r}{2}}$$

The **integrated cross section** is given by

$$\sigma(E_\nu) = \int_0^{E_r^{\max}(E_\nu)} \frac{d\sigma(E_\nu, E_r)}{dE_r} dE_r$$

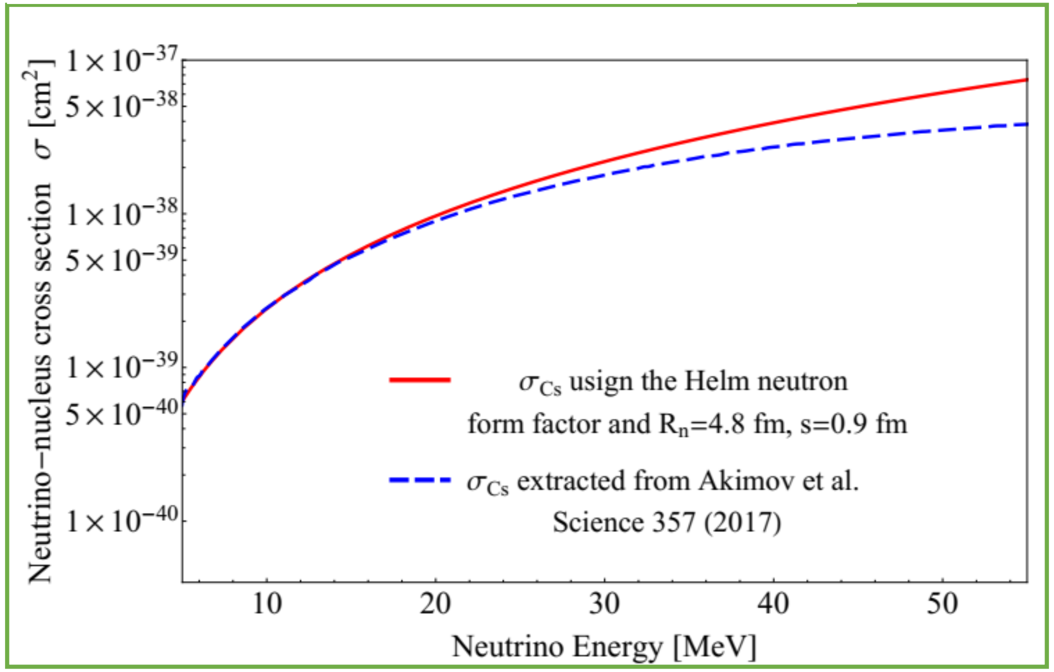

In the case of the COHERENT experiment, the coherent elastic scattering is measured on Cs and I, which contribute incoherently, leading to the **total cross section**

$$\boxed{\frac{d\sigma_{\nu-CsI}}{dE_r} = \frac{d\sigma_{\nu-Cs}}{dE_r} + \frac{d\sigma_{\nu-I}}{dE_r}}$$

With the already discussed approximation

$$F_{N,\mathrm{Cs}}(q^2) \simeq F_{N,\mathrm{I}}(q^2) \simeq F_N(q^2)$$

Fitting the COHERENT data: Acceptance efficency

The theoretical number of CEnNS events in each energy bin *i* **depends on the neutron form factor** and it is given by

$$N_i^{th} = N_{CsI} \int_{E_{r_i}}^{E_{r_{i+1}}} dE_r \int_{E_{min}} dE_\nu \boxed{A(E_r)} \boxed{\frac{dN_\nu}{dE_\nu}} \boxed{\frac{d\sigma_{\nu-CsI}}{dE_r}}$$

The processing and analysis of the CsI data imposed an acceptance efficiency in terms of the photoelectron content of the signal *x*

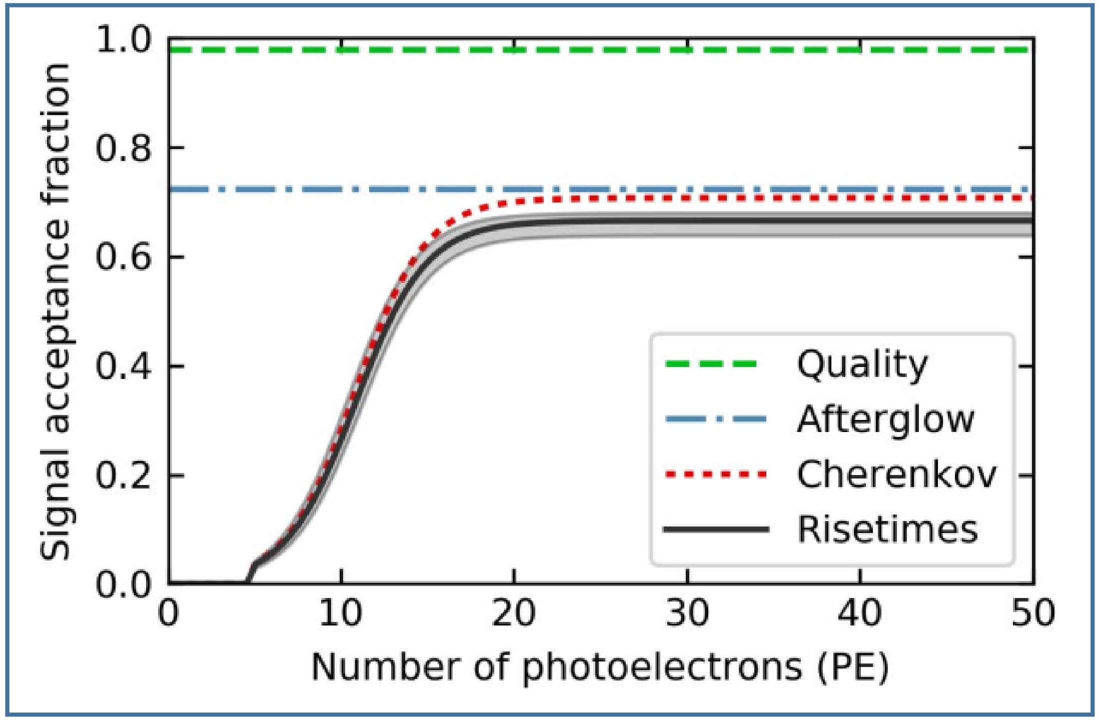

$$f(x) = \frac{a}{1+\exp\left(-k\left(x-x_0\right)\right)}\Theta(x-5)$$

where Θ(*x*) is a modified Heaviside step function and the parameters have values

$$a = 0.6655^{+0.0212}_{-0.0384}, \quad k = 0.4942^{+0.0335}_{-0.0131}, \quad x_0 = 10.8507^{+0.1838}_{-0.3995}$$

$$\Theta(x) = \begin{cases} 0 & x < 5, \\ 0.5 & 5 \leq x < 6, \\ 1 & x \geq 6. \end{cases}$$

[10] B.J. Scholz. *First observation of coherent elastic neutrino-nucleus scattering*. Ph.D. thesis, University of Chicago (2017).
[11] COHERENT Collaboration data release, arXiv:1804.09459v1 [nucl-ex]
[12] D. Akimov *et al.* “Observation of coherent elastic neutrino-nucleus scattering." *Science* **357**, 1123-1126 (2017). 1708.01294.

Fitting the COHERENT data: neutrino flux

The theoretical number of CEnNS events in each energy bin *i* **depends on the neutron form factor** and it is given by

$$N_i^{th} = N_{CsI} \int_{E_{r_i}}^{E_{r_{i+1}}} dE_r \int_{E_{min}} dE_\nu \boxed{A(E_r)} \boxed{\frac{dN_\nu}{dE_\nu}} \boxed{\frac{d\sigma_{\nu-CsI}}{dE_r}}$$

The total **neutrino flux** is composed of

- Prompt ν_μ component from stopped pion decays
- Two delayed components of $\bar{\nu}_\mu$ and ν_e from muon decays

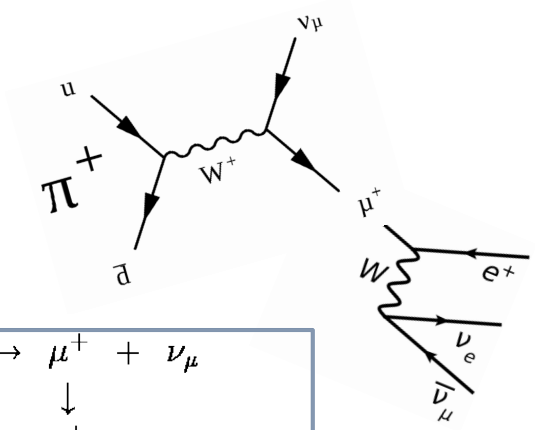

$$\begin{array}{l} \pi^+ \to \mu^+ + \nu_\mu \\ \qquad\;\; \downarrow \\ \qquad\;\; e^+ + \nu_e + \bar{\nu}_\mu \end{array}$$

$$\frac{dN_{\nu_\mu}}{dE_\nu} = \eta\,\delta\left(E_\nu - \frac{m_\pi^2 - m_\mu^2}{2m_\pi}\right),$$

$$\frac{dN_{\nu_{\bar{\mu}}}}{dE_\nu} = \eta\,\frac{64E_\nu^2}{m_\mu^3}\left(\frac{3}{4} - \frac{E_\nu}{m_\mu}\right),$$

$$\frac{dN_{\nu_e}}{dE_\nu} = \eta\,\frac{192E_\nu^2}{m_\mu^3}\left(\frac{1}{2} - \frac{E_\nu}{m_\mu}\right),$$

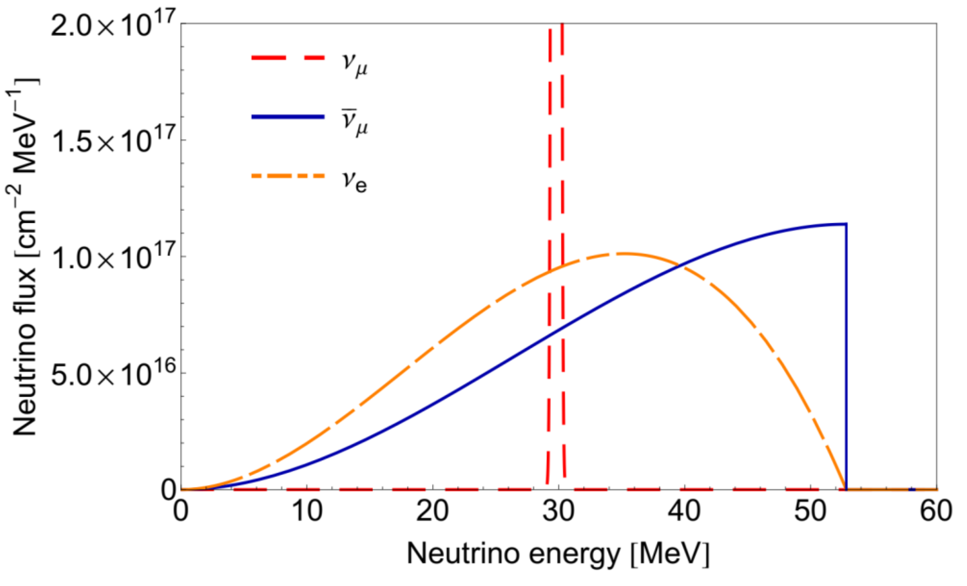

$E_\nu \leq m_\mu/2 \cong 52.8$ MeV, with the normalization factor $\eta = rN_{POT}/4\pi L^2$, where r = 0.08 is the number of neutrinos per flavor that are produced for each proton on target, $N_{POT} = 1.76 \times 10^{23}$ is the number of proton on target and L = 19.3 m is the distance between the source and the COHERENT detector.

Fitting the COHERENT data: last ingredients

The theoretical number of CEnNS events in each energy bin *i* **depends on the neutron form factor** and it is given by

$$N_i^{th} = \boxed{N_{CsI}} \int_{E_{r_i}}^{E_{r_{i+1}}} dE_r \int_{E_{min}} dE_\nu \boxed{A(E_r)} \boxed{\frac{dN_\nu}{dE_\nu}} \boxed{\frac{d\sigma_{\nu-CsI}}{dE_r}}$$

N_{CsI} is the number of CsI in the detector given by $N_A M_{det}/M_{CsI}$, where N_A is the Avogadro number, M_{det} = 14.6 kg, is the detector mass, and M_{CsI} = 259.8 is the molar mass of CsI.

We considered only the **12 energy bins from *i* = 4 to *i* = 15** for which the COHERENT Collaboration fitted the **quenching factor** obtaining the linear relation between the observed number of photoelectrons N_{PE} and the nuclear kinetic recoil energy E_r given by

$$\boxed{N_{\mathrm{PE}} = 1.17 \left(\frac{E_r}{\mathrm{keV}}\right)}$$

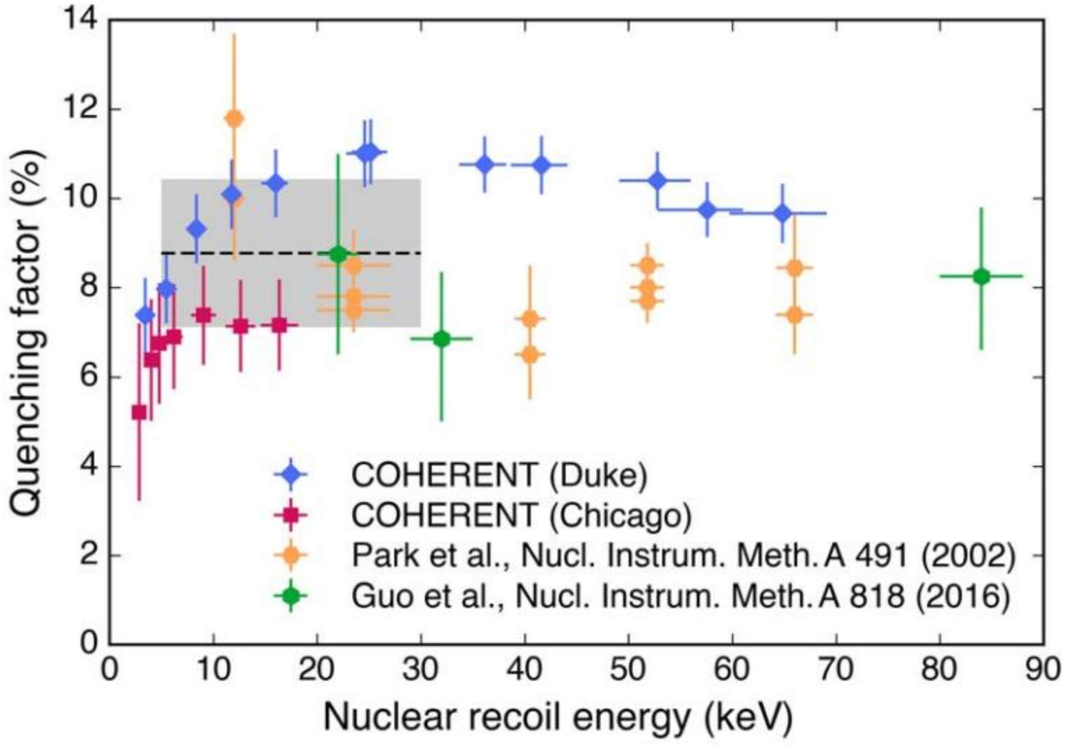

The χ^2 definition

To fit the data the following χ^2 has been defined

$$\chi^2 = \sum_{i=4}^{15} \left(\frac{N_i^{\mathrm{exp}} - (1+\alpha)N_i^{\mathrm{th}} - (1+\beta)B_i}{\sigma_i} \right)^2 + \left(\frac{\alpha}{\sigma_\alpha} \right)^2 + \left(\frac{\beta}{\sigma_\beta} \right)^2 .$$

- For each energy bin *i*, N_i^{exp} and N_i^{th} are, respectively, the experimental and theoretical number of events, $\boldsymbol{B_i}$ **is the estimated number of background** events and $\boldsymbol{\sigma_i}$ **is the statistical uncertainty**.

- α and β are **nuisance parameters** for the systematic uncertainties of the signal rate and of the background rate, respectively. The corresponding standard deviations are σ_α = 0.28 and σ_β = 0.25.

First average CsI neutron density distribution measurement

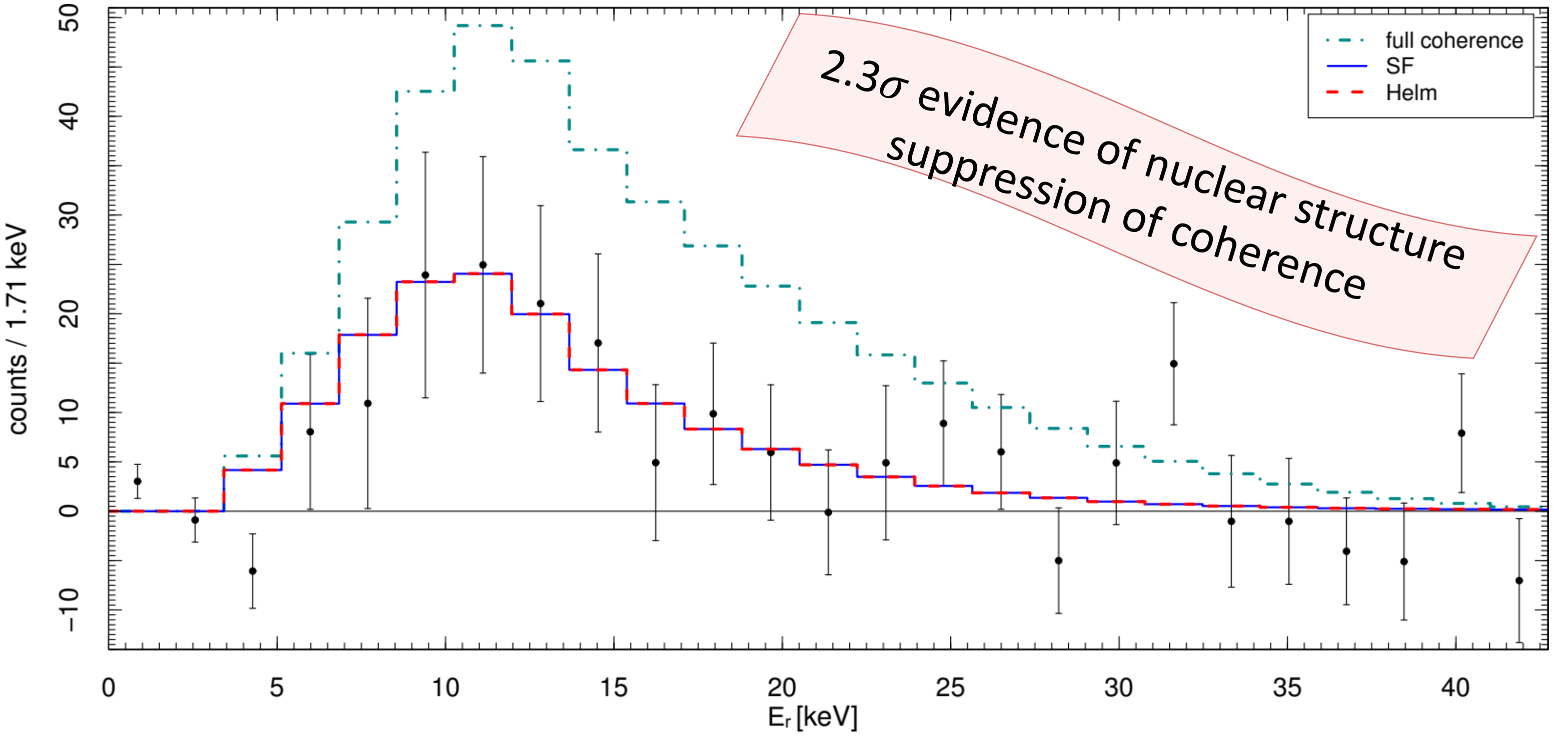

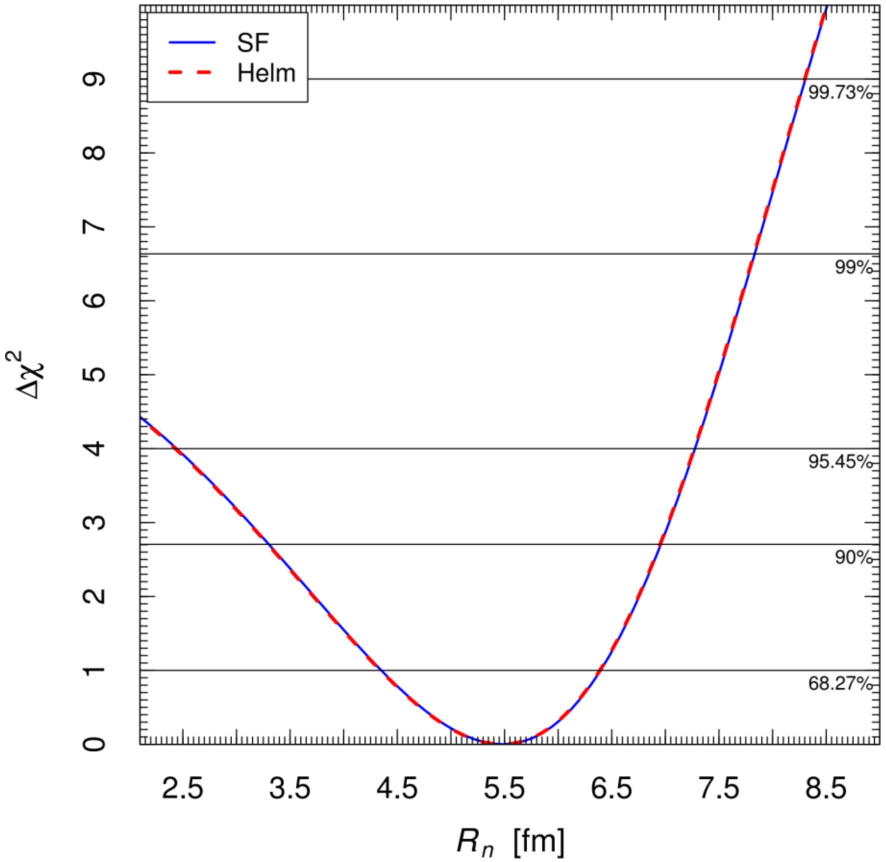

- We first compared the data with the predictions in the case of full coherence, i.e. all nuclear form factors equal to unity: **the corresponding histogram does not fit the data**.
- We fitted the COHERENT data in order to get information on the value of the neutron rms radius R_n, which is **determined by the minimization of the χ^2** using the **symmetrized Fermi** and **Helm form factors**.

This is the first model independent measurement of the CsI neutron radius

$$R_n^{CsI} = 5.5^{+0.9}_{-1.1}\ \text{fm}$$

The neutron skin

$$R_n^{CsI} = 5.5_{-1.1}^{+0.9}\ \text{fm}$$

Proton rms radius for Cs and I

$R_p^{Cs} = 4.804$ fm and
$R_p^{I} = 4.749$ fm
are around 4.78 fm, with a difference of about 0.05 fm

The neutron skin

$$\Delta R_{np}^{CsI} \equiv R_n - R_p \cong 0.7_{-1.1}^{+0.9}\ \text{fm}$$

Theoretical values of the proton and neutron rms radii of Cs and I obtained with nuclear mean field models. The value is compatible with all the models...

	^{133}Cs			^{127}I			CsI		
Model	R_p	R_n	$R_n - R_p$	R_p	R_n	$R_n - R_p$	R_p	R_n	$R_n - R_p$
SHF SkM* [20]	4.76	4.90	0.13	4.71	4.84	0.13	4.73	4.86	0.13
SHF SkP [21]	4.79	4.91	0.12	4.72	4.84	0.12	4.75	4.87	0.12
SHF SkI4 [22]	4.73	4.88	0.15	4.67	4.81	0.14	4.70	4.83	0.14
SHF Sly4 [23]	4.78	4.90	0.13	4.71	4.84	0.13	4.73	4.87	0.13
SHF UNEDF1 [24]	4.76	4.90	0.15	4.68	4.83	0.15	4.71	4.87	0.15
RMF NL-SH [25]	4.74	4.93	0.19	4.68	4.86	0.19	4.71	4.89	0.18
RMF NL3 [26]	4.75	4.95	0.21	4.69	4.89	0.20	4.72	4.92	0.20
RMF NL-Z2 [27]	4.79	5.01	0.22	4.73	4.94	0.21	4.76	4.97	0.21

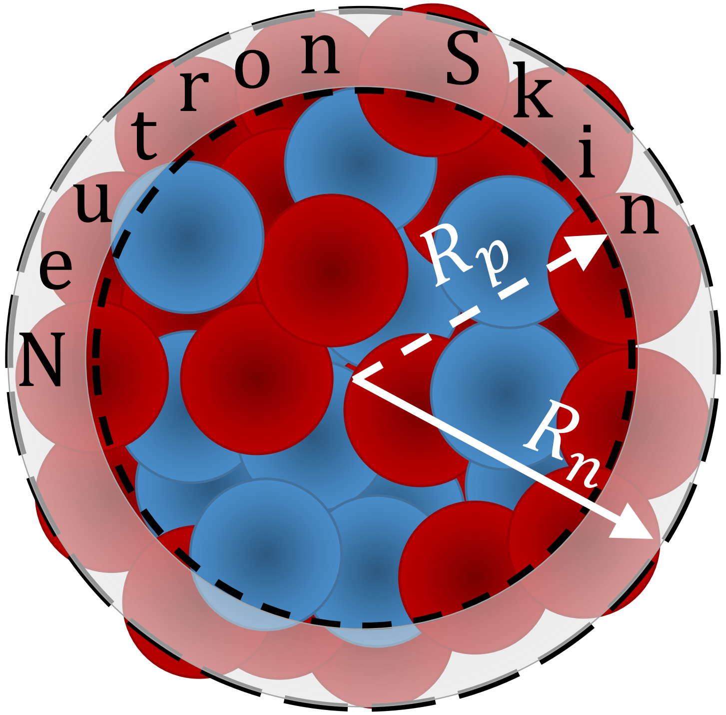

... but the central value tends to favour models that predict a larger value of R_n.

Cs neutron radius and implications

Upcoming direct dark matter detection experiments will have sensitivity to detect neutrinos from several astrophysical sources (Sun, atmosphere, and diffuse Supernovae)

Information on R_n is important for a precise determination of the background due to CEnNS in dark matter detectors. This background will crucially limit the discovery potential [13]. Until now, this background has been evaluated using a unique Helm nuclear form factor for protons and neutrons, with the Lewin-Smith prescription [4] for the input value of the nuclear radii. Since Cs and I have similar atomic and mass numbers to that of Xenon (A=131, Z=54), we can estimate **the impact of the inclusion of different proton and neutron form factors** (with the value of R_n found in our paper) on the neutrino background for experiments like DARWIN [14], XENONnT [15], and LZ [16], that use Xenon as a target.

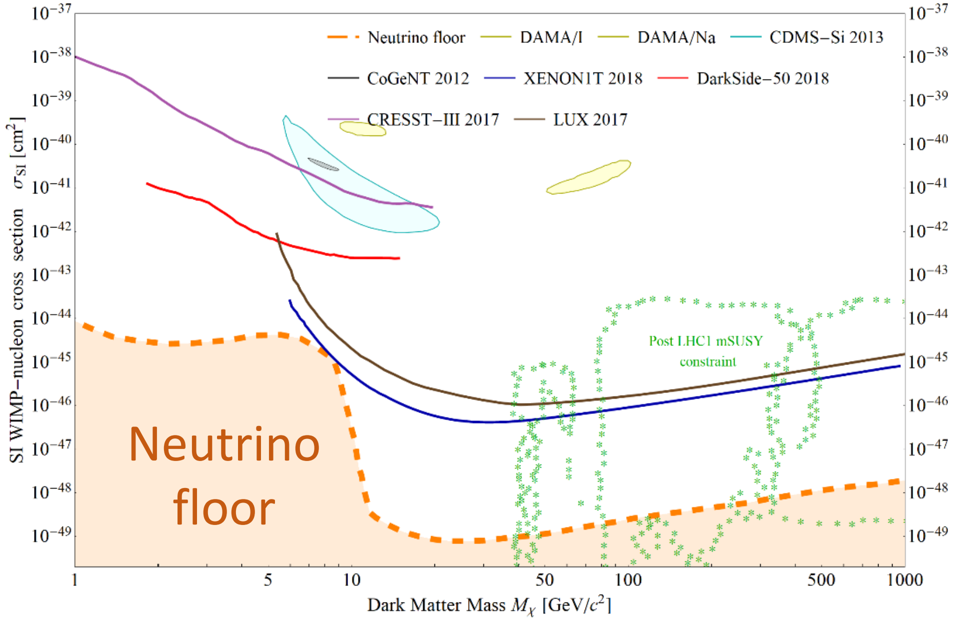

Ratio between the differential cross-section with a unique Helm nuclear form factor (in the Lewin Smith parametrization) and that including the neutron form factor with $R_n \approx 5.5$ *fm.*

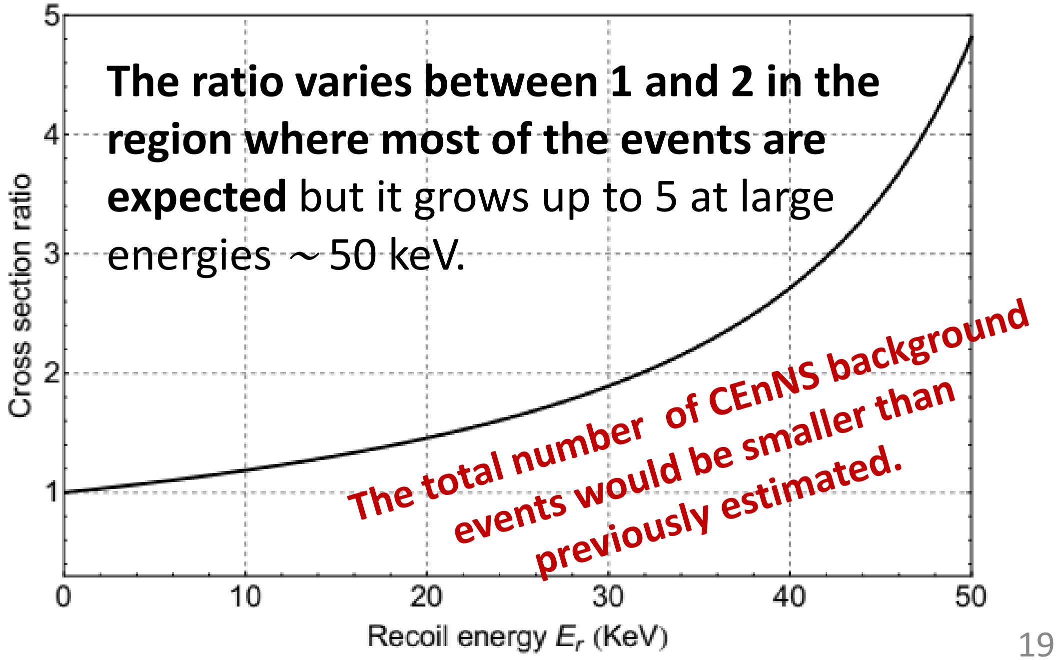

[13] Billard et al. PRD 89, 023524 (2015)
[14] J. Aalbers *et al.*, JCAP **1611**, 017 (2016)
[15] E. Aprile *et al.* (XENON), JCAP **1604**, 027 (2016)
[16] B. J. Mount *et al.*, arXiv:1703.09144 [physics.ins-det]

Conclusions

NEUTRON DISTRIBUTION INFORMATION USING CEnNS

- **A novel way to measure the neutron distribution has been proposed**
- Analysing the COHERENT data, the **first determination of the average neutron distribution radius of Cs and I** has been obtained. The **practically model-independent value of $R_n = 5.5^{+0.9}_{-1.1}$ fm has been derived**.
- Moreover, the COHERENT data show a **2.3σ evidence of the nuclear structure suppression of the full coherence**.
- The difference between the neutron and proton rms radii, the "neutron skin", has been derived: **$R_n - R_p \cong 0.7^{+0.9}_{-1.1}$ fm.** The best-fit value indicates the possibility of a value that is larger than the model-predicted values which lies between about 0.1 and 0.3 fm.

This study has many consequences for direct dark matter searches and also for nuclear physics models and for the equation of state of neutron stars!

Thanks for your attention

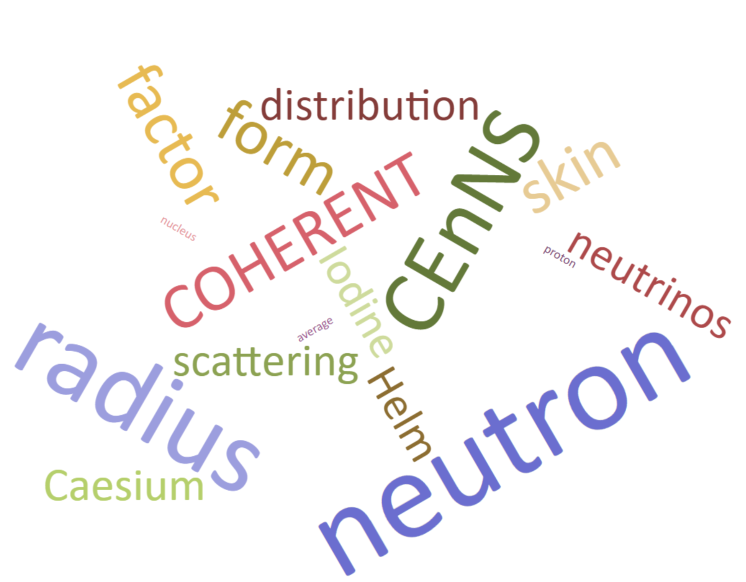

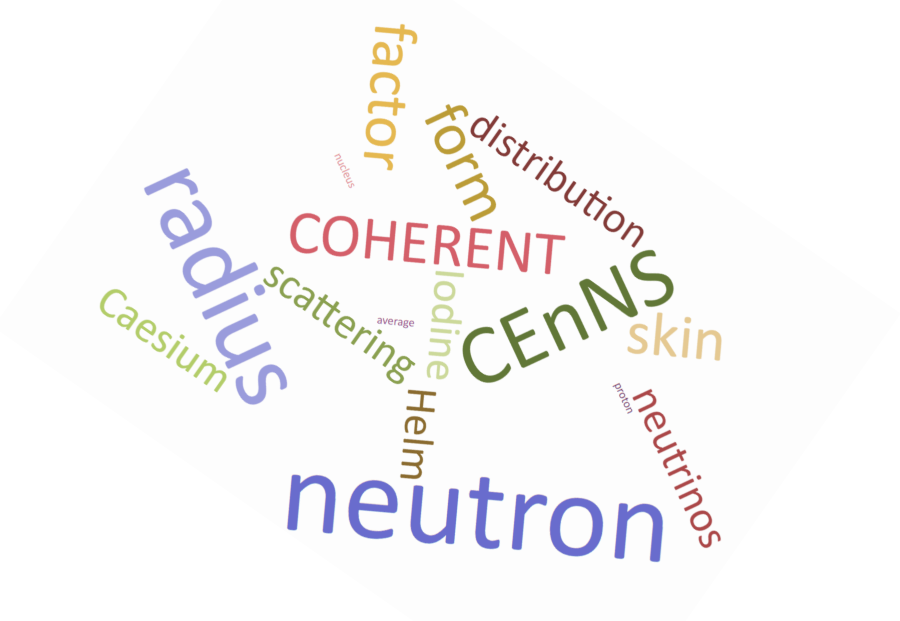

BACKUP

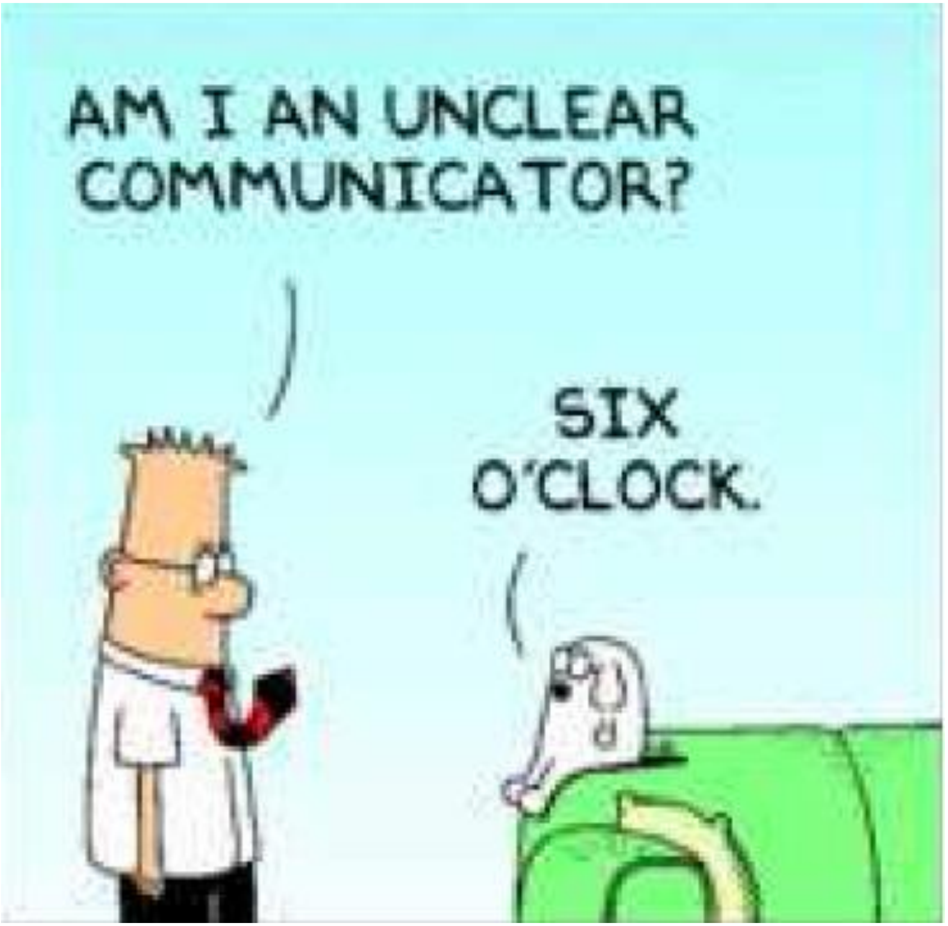

Projection for R_n measurement

Future data of the COHERENT experiment may lead to a better determination of the neutron rms radius R_n and of the neutron skin ΔR_{np}. Figure shows the estimation of the sensitivity to R_n of the COHERENT experiment as a function of the number of protons on target with **the current systematic uncertainties**, with **half the current systematic uncertainties**, and with **one-quarter of the current systematic uncertainties**, including the effect of the beam-off background.

- With the **current systematic uncertainties** and **10 times the current number of N_{POT}**, the data of the COHERENT experiment will allow us to determine **R_n within about 0.5 fm**.

- If the systematic uncertainties are reduced by half or one-quarter, $\boldsymbol{R_n}$ can be determined within about **0.4** or **0.3 fm**, respectively.

The current sensitivity gives a relative uncertainty $\Delta R_n / R_n \simeq 17\%$, which is in approximate agreement with the uncertainty of our determination of R_n.

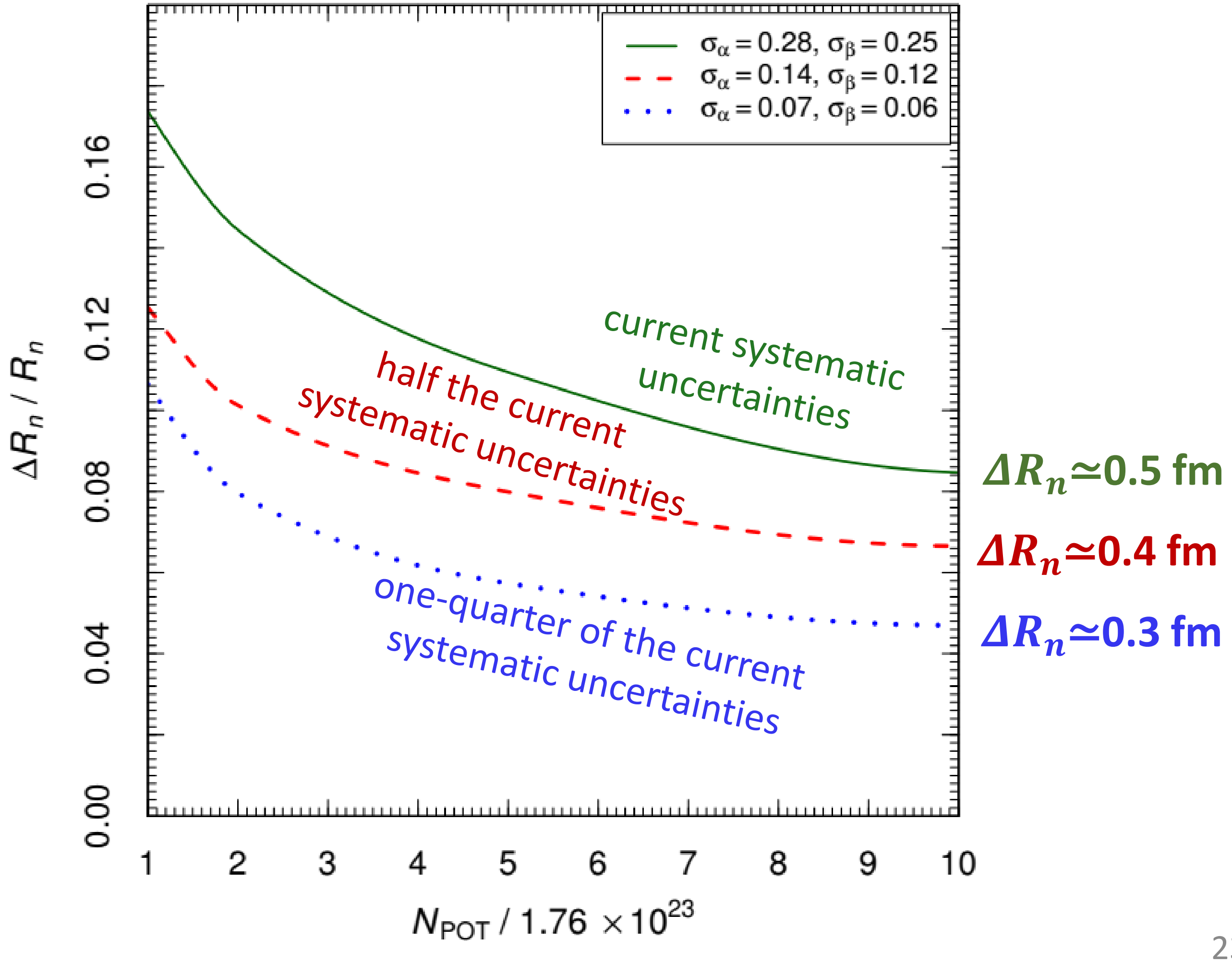

Neutron skin and implications


Selected for a Viewpoint in *Physics*
PRL **119,** 161101 (2017) PHYSICAL REVIEW LETTERS week ending 20 OCTOBER 2017

GW170817: Observation of Gravitational Waves from a Binary Neutron Star Inspiral

B. P. Abbott *et al.**

(LIGO Scientific Collaboration and Virgo Collaboration)

(Received 26 September 2017; revised manuscript received 2 October 2017; published 16 October 2017)

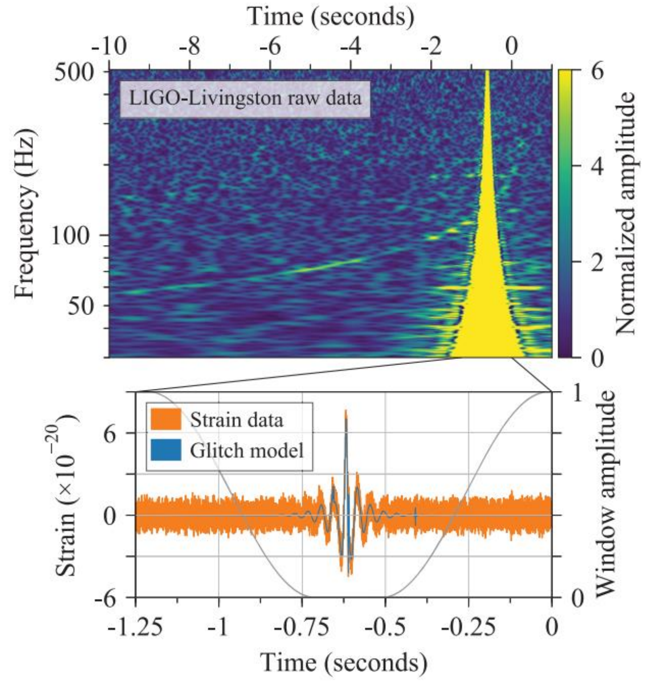

On August 17, 2017 the Advanced LIGO and Advanced Virgo gravitational-wave detectors made their **first observation of a binary neutron star inspiral**.

The collaboration was able to infer also the tidal deformability parameter, **which is related to the neutron star equation of state and to the neutron skin**

$$\tilde{\Lambda} = \frac{16}{13}\frac{(m_1 + 12m_2)m_1^4\Lambda_1 + (m_2 + 12m_1)m_2^4\Lambda_2}{(m_1 + m_2)^5}$$

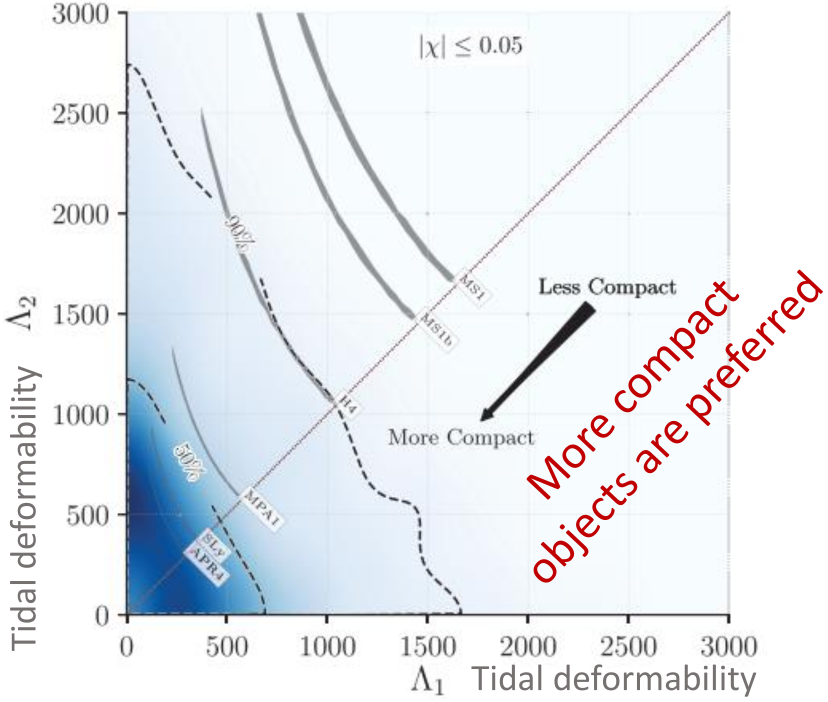

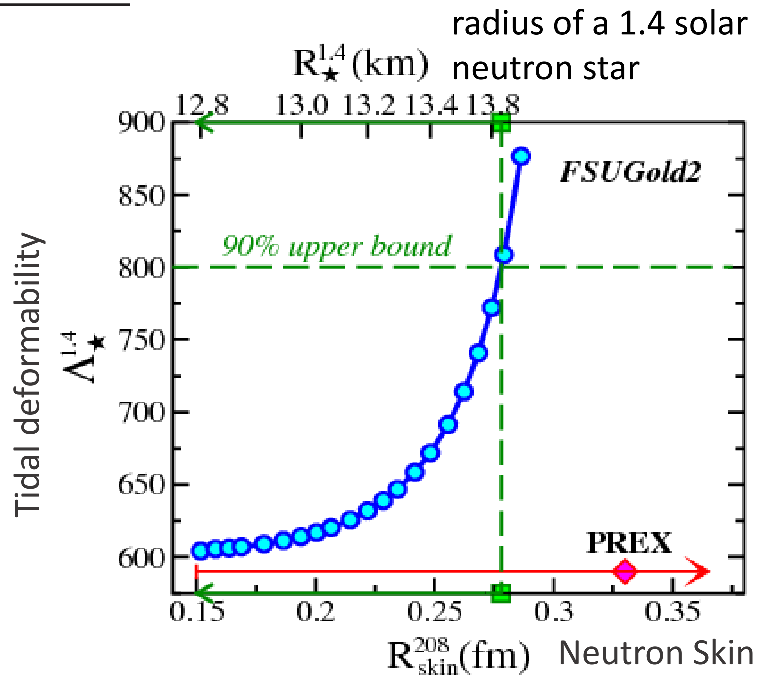

Fattoyev et al. "*Neutron skins and neutron stars in the multi-messenger era*", Phys. Rev. Lett. **120**, 172702

Why is Coherent neutrino Nucleus scattering interesting?

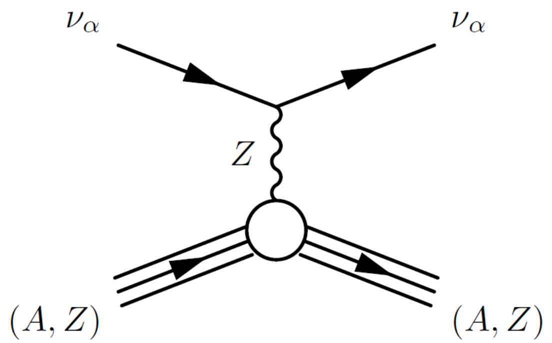

- Differences from Standard-Model prediction could be a sign of new physics
- Supernova process (Supernova evolution: Coherent neutrino scattering ($\sigma \sim A^2$) may push heavy elements to the outer shell of the star (Rev. Nucl. Part. Sci 27 167, 1977)
- Supernova neutrino detection (Supernova neutrino detection: ~10 neutrino-nucleus coherent events on argon in a 10 second window per ton for a galactic supernova at 10 kpc. Important info about ν_μ and ν_τ that is out of reach for Water Cerenkov)
- Weak mixing angle (The weak mixing angle can be found by measuring the absolute cross-section. A cross section measurement with ~ 10% uncertainty gives a uncertainty of ~ 5% at low Q values. Canas et al. PLB, 784, 159-163 (Arxiv:1806.01310))
- Non-standard neutrino interactions (The signature of NSI is a deviation from the expected cross section. See Barranco, et al. PRD 76, 073008, Arxiv:0702175 (2007)] for specific NSI new physics possibilities from a neutrino-nucleus coherent measurement (extra neutral gauge bosons, leptoquarks, and R-parity breaking interactions)
- Sterile neutrinos
- Dark Matter direct detection (irriducible background)

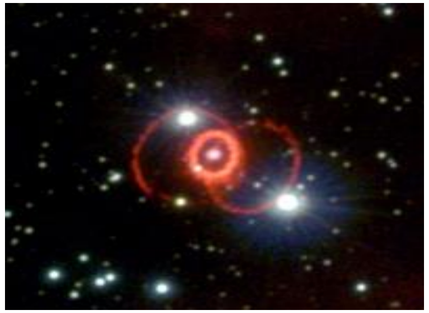

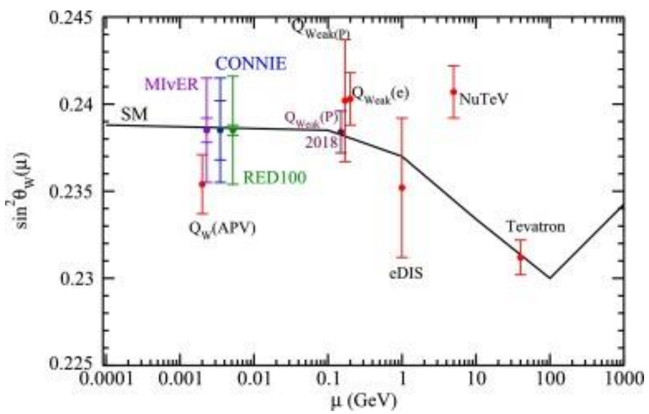

- Unique probe of the neutron distribution inside a nucleus (this talk)

Neutron form factor parametrization

1. **Symmetrized Two-parameter Fermi form factor** $\rho_{SF}(r) = \rho_F(r) + \rho_{SF}(-r) - 1$ with $\rho_F(r) = \dfrac{\rho_0}{1 + e^{(r-c)/a}}$

Neutron rms radius →

$$R_n^2 = \frac{3}{5}c^2 + \frac{7}{5}(\pi a)^2.$$

$$F_Z^{\mathrm{SF}}(q^2) = \frac{3}{qc\left[(qc)^2 + (\pi qa)^2\right]}\left[\frac{\pi qa}{\sinh(\pi qa)}\right] \times \left[\frac{\pi qa \sin(qc)}{\tanh(\pi qa)} - qc\cos(qc)\right].$$

2. **Helm form factor**

Neutron rms radius →

The Helm FF is defined as the product of two fairly simple form factors: one associated with a uniform (box) density F_B and the other one accounting for a Gaussian falloff F_G

$$F_{\mathrm{H}}(q) = F_{\mathrm{B}}(q)F_{\mathrm{G}}(q) = 3\,\frac{j_1(qR_0)}{qR_0}e^{-q^2 s^2/2}$$

$$F_{\mathrm{B}}(q) = \int e^{-i\mathbf{q}\cdot\mathbf{r}}\rho_{\mathrm{B}}(r)d^3r = \int e^{-i\mathbf{q}\cdot\mathbf{r}}\left(\frac{3\Theta(R_0 - r)}{4\pi R_0^3}\right)d^3r = 3\,\frac{j_1(qR_0)}{qR_0}$$

$$F_{\mathrm{G}}(q) = \int e^{-i\mathbf{q}\cdot\mathbf{r}}\rho_{\mathrm{G}}(r)d^3r = \int e^{-i\mathbf{q}\cdot\mathbf{r}}\left(\frac{e^{-r^2/(2s^2)}}{(2\pi s^2)^{3/2}}\right)d^3r = e^{-q^2 s^2/2}.$$

Helm form factor

The Helm FF is defined as the product of two fairly simple form factors: one associated with a uniform (box) density F_B and the other one accounting for a Gaussian falloff F_G

$$F_{\rm H}(q) = F_{\rm B}(q)F_{\rm G}(q) = 3\,\frac{j_1(qR_0)}{qR_0}e^{-q^2 s^2/2}$$

$$F_{\rm B}(q) = \int e^{-i\mathbf{q}\cdot\mathbf{r}}\rho_{\rm B}(r)d^3r = \int e^{-i\mathbf{q}\cdot\mathbf{r}}\left(\frac{3\Theta(R_0-r)}{4\pi R_0^3}\right)d^3r = 3\,\frac{j_1(qR_0)}{qR_0}$$

$$F_{\rm G}(q) = \int e^{-i\mathbf{q}\cdot\mathbf{r}}\rho_{\rm G}(r)d^3r = \int e^{-i\mathbf{q}\cdot\mathbf{r}}\left(\frac{e^{-r^2/(2\,s^2)}}{(2\pi\,s^2)^{3/2}}\right)d^3r = e^{-q^2 s^2/2}\,.$$

Here, Θ is the Heaviside function and $j1(x)$ is the spherical Bessel function of order one

$$j_1(x) = \frac{\sin(x)}{x^2} - \frac{\cos(x)}{x}$$

A great advantage of the Helm form factor is that it is defined in terms of a form factor that encodes the uniform interior density and another one that characterizes the nuclear surface. As a consequence, the Helm form factor is defined entirely in terms of two constants the box (or "diffraction") radius R_0 and the surface thickness s, parameters that need to be fit separately for each nucleus. A closed form expression for the Helm density exists and it is given by

$$\rho_{\rm H}(r) = \frac{1}{2}\rho_0\left[\mathrm{erf}\left(\frac{r+R_0}{\sqrt{2}\,s}\right) - \mathrm{erf}\left(\frac{r-R_0}{\sqrt{2}\,s}\right)\right] + \frac{1}{\sqrt{2\pi}}\left(\frac{s}{r}\right)\rho_0\left[\exp\left(-\frac{(r+R_0)^2}{2\,s^2}\right) - \exp\left(-\frac{(r-R_0)^2}{2\,s^2}\right)\right]$$

$$\rho_0 \equiv \frac{3}{4\pi R_0^3}$$

The first three moments of the Helm distribution are given by

$$R^2 \equiv \langle r^2\rangle = \frac{3}{5}R_0^2 + 3s^2\,,$$

$$R^4 \equiv \langle r^4\rangle = \frac{3}{7}R_0^4 + 6R_0^2 s^2 + 15s^4\,,$$

$$R^6 \equiv \langle r^6\rangle = \frac{1}{3}R_0^6 + 9R_0^4 s^2 + 63R_0^2 s^4 + 105s^6$$

The COHERENT collaboration prescription

1. **Symmetrized Two-parameter Fermi form factor** $\rho_{SF}(r) = \rho_F(r) + \rho_{SF}(-r) - 1$ with $\rho_F(r) = \dfrac{\rho_0}{1 + e^{(r-c)/a}}$

Neutron rms radius

$$R_n^2 = \frac{3}{5}c^2 + \frac{7}{5}(\pi a)^2.$$

$$F_Z^{\mathrm{SF}}(q^2) = \frac{3}{qc\left[(qc)^2 + (\pi qa)^2\right]}\left[\frac{\pi qa}{\sinh(\pi qa)}\right] \times \left[\frac{\pi qa \sin(qc)}{\tanh(\pi qa)} - qc\cos(qc)\right].$$

2. **Klein form factor**

$$F(q^2) = \frac{4\pi\rho_0}{Aq^3}\left[\sin(qR_a) - qR_a\cos(qR_A)\right]\left[\frac{1}{1+a^2q^2}\right].$$

The collaboration uses a unique nuclear form factor for neutrons and protons (one for Cs and one for I) as described in [1]. The Klein FF (see Fig. 7.5) is an approximation of the the Woods-Saxon distribution as a hard sphere, with radius R_A, convoluted with a Yukawa potential with range r = 0.7 fm.

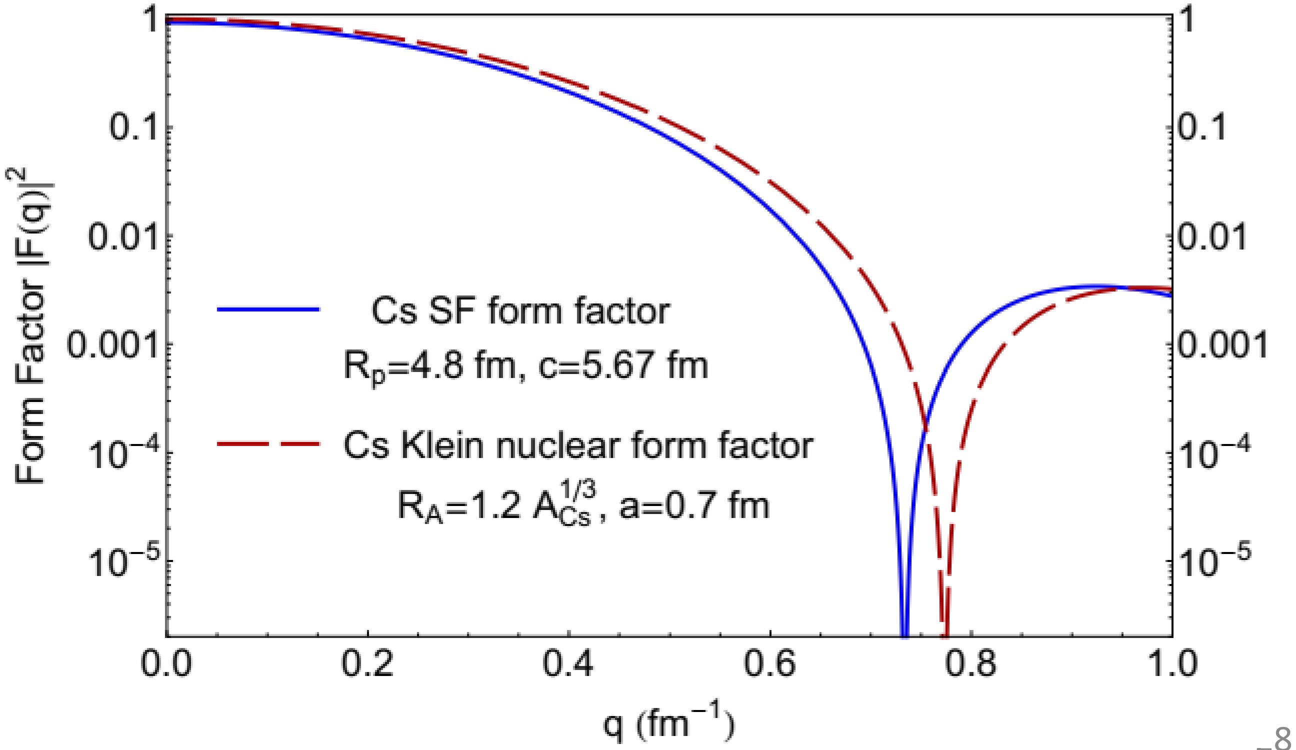

[1] Spencer Klein and Joakim Nystrand. *Phys. Rev.* C60 (1999), p. 014903. arXiv:hep-ph/9902259 [hep-ph]

Neutron density distribution

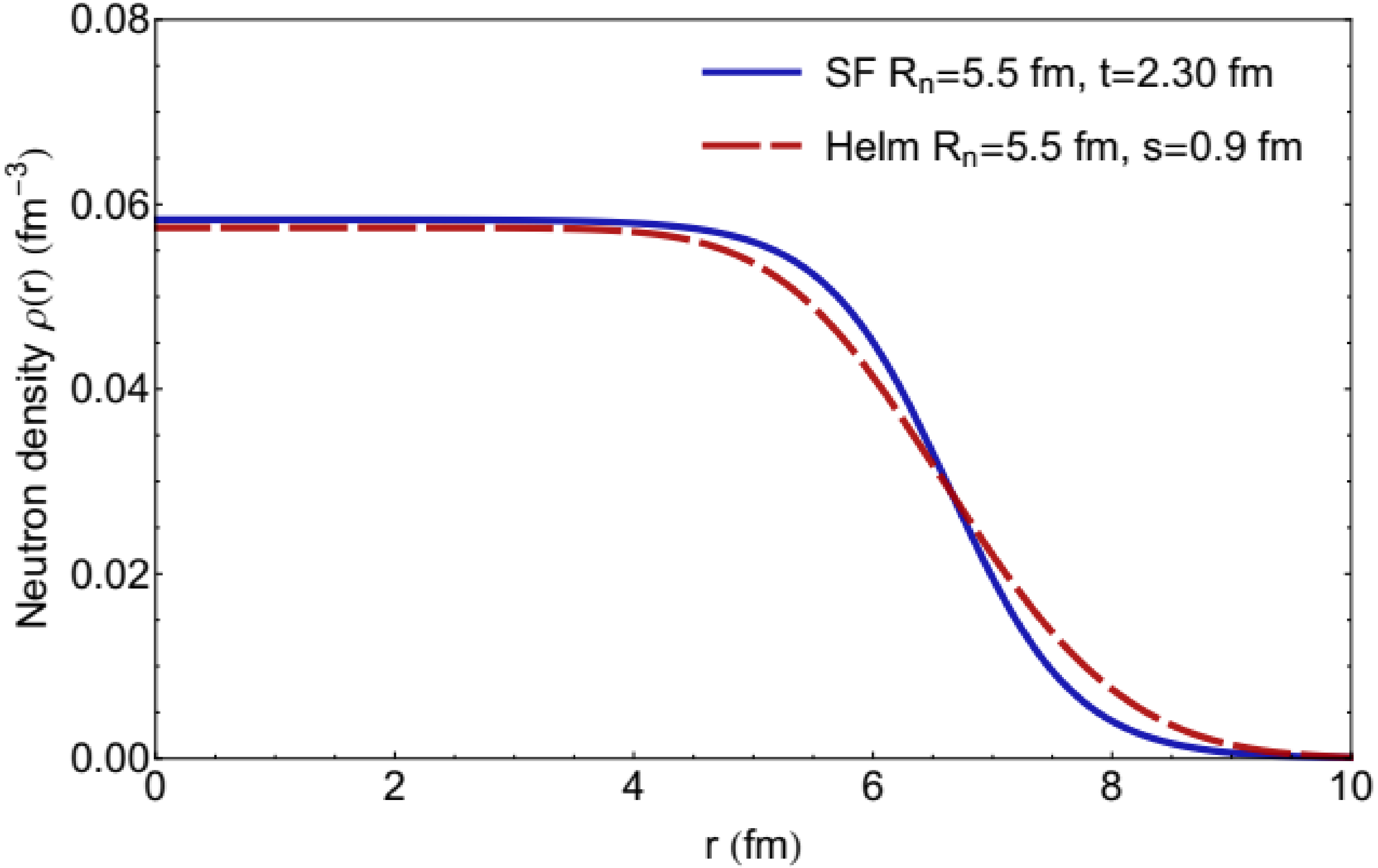

The proton structures of Cs and I have been studied with muonic atom spectroscopy

TABLE IIIA. Muonic $2p \rightarrow 1s$ Transition Energies and Barrett Radii for $Z < 60$ and $Z > 77$

See page 194 for Explanation of Tables

Isotope	$E_{exp.}$ [keV]	$E_{theo.}$ [keV]	NPol [keV]	c [fm]	$\langle r^2 \rangle^{1/2}_{model}$ [fm]	α [1/fm]	k	C_z [am/keV]	$R^{\mu}_{k\alpha}$ [fm]	Ref.
^{133}Cs	3840.702	3840.670	1.531			0.1193	2.2296	-2.759	6.1459	[Kl88]
	39			5.6710	4.804				(1;13)	
	3902.636	3902.656	1.289	1		0.1182	2.2274	-2.710	6.1464	
	31								(1;11)	
^{127}J	3667.361	3667.466	0.532			0.1166	2.2229	-2.969	6.0762	[Kl88]
	35			5.5931	4.749				(1;5)	
	3723.742	3723.650	1.454	1		0.1155	2.2209	-2.919	6.0768	
	33								(1;13)	

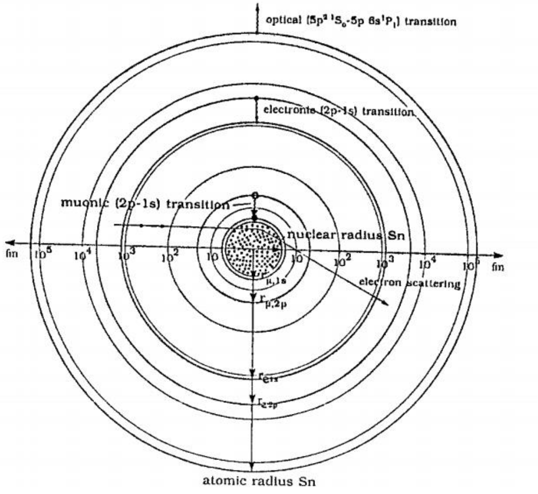

Fig. 1. Sensibilities of elastic electron scattering, muonic atom x-rays, electronic x-rays and optical transitions to the finite nuclear charge extension for the example of the tin atom. Note the logarithmic length scale.

The proton structures of Cs and I have been studied with muonic atom spectroscopy

Starting point for the calculations of all muonic atom energy levels is the Dirac point nucleus approximation. In intermediate muonic states, the muon-nucleus system is almost hydrogenlike, and the approximation is good. ***Near the nucleus however, the finite nuclear charge size may lower the muonic binding energy by as much as 50%.*** Hence, the Dirac equation has to be numerically solved, using a static central potential with adjustable nuclear charge parameters. Due to the double integration procedure, the exact form of the chosen nuclear charge distribution (**usually a two-parameter Fermi distribution**) does not influence the final result in an appreciable way.

Due to the large overlap of the innermost muonic wave functions with the nuclear charge density in all but the lightest nuclei, nuclear ground state moments and their 'fine structures' in terms of isotope or isotone shifts can be determined with high precision. By means of hyperfine structure splittings, magnetic dipole moments and electric quadrupole moments of the nuclear ground states can be measured

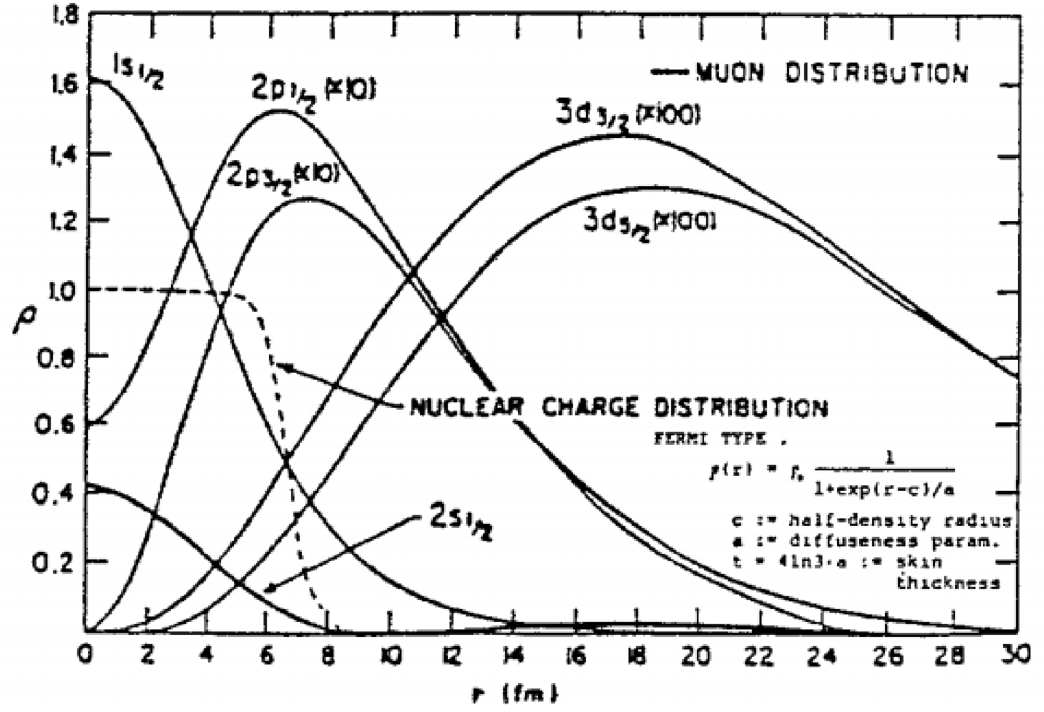

Fig. 2. Overlap of the muon probability densities $|\psi|^2$ of the innermost states with the nuclear charge density ρ in the case of $\mu^- - {}^{208}Pb$.

From L. A. Schaller, Muonic atoms spectroscopy Zeitschrift für Physik C Particles and Fields 1992, Volume 56, Supplement 1, pp S48–S58

Prompt neutron background

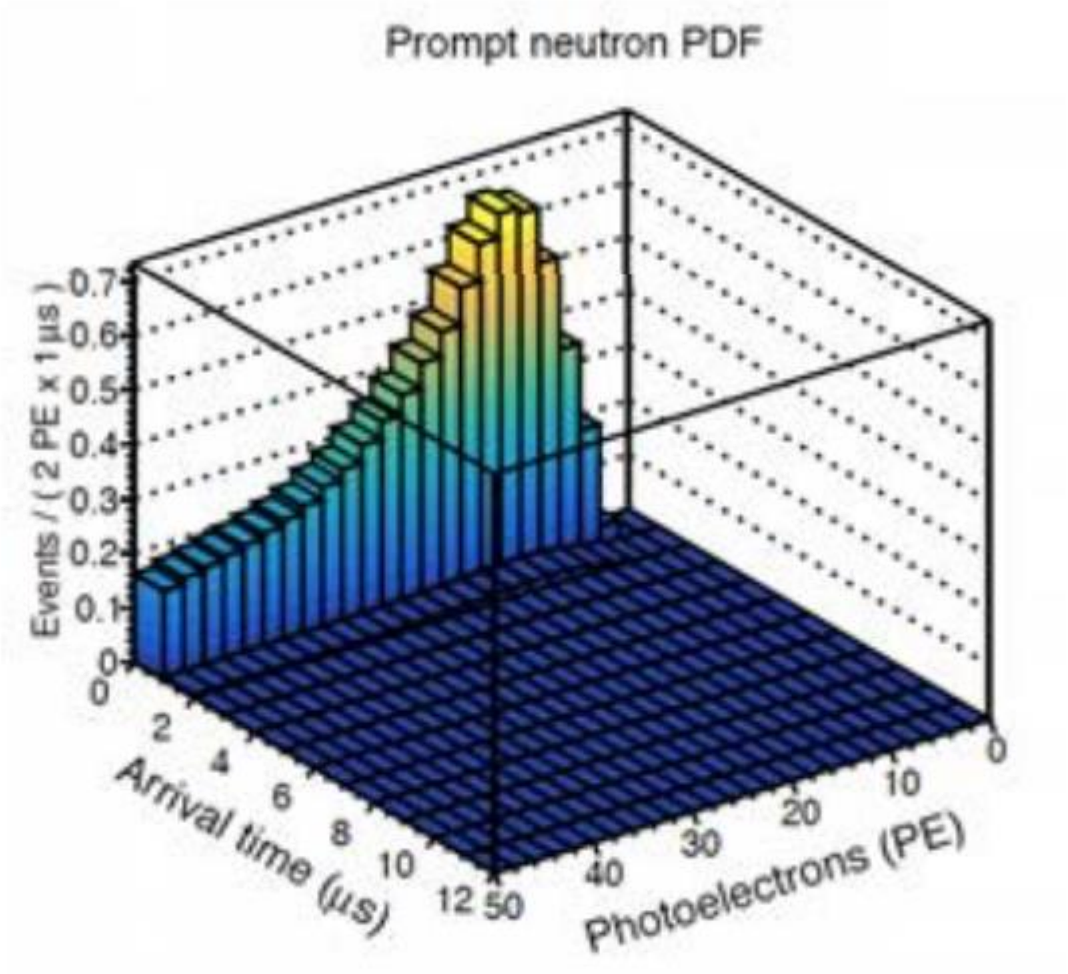

[5] D. Akimov et al. "Observation of Coherent Elastic Neutrino-Nucleus Scattering" ***Science*** *357.6356 (2017)*

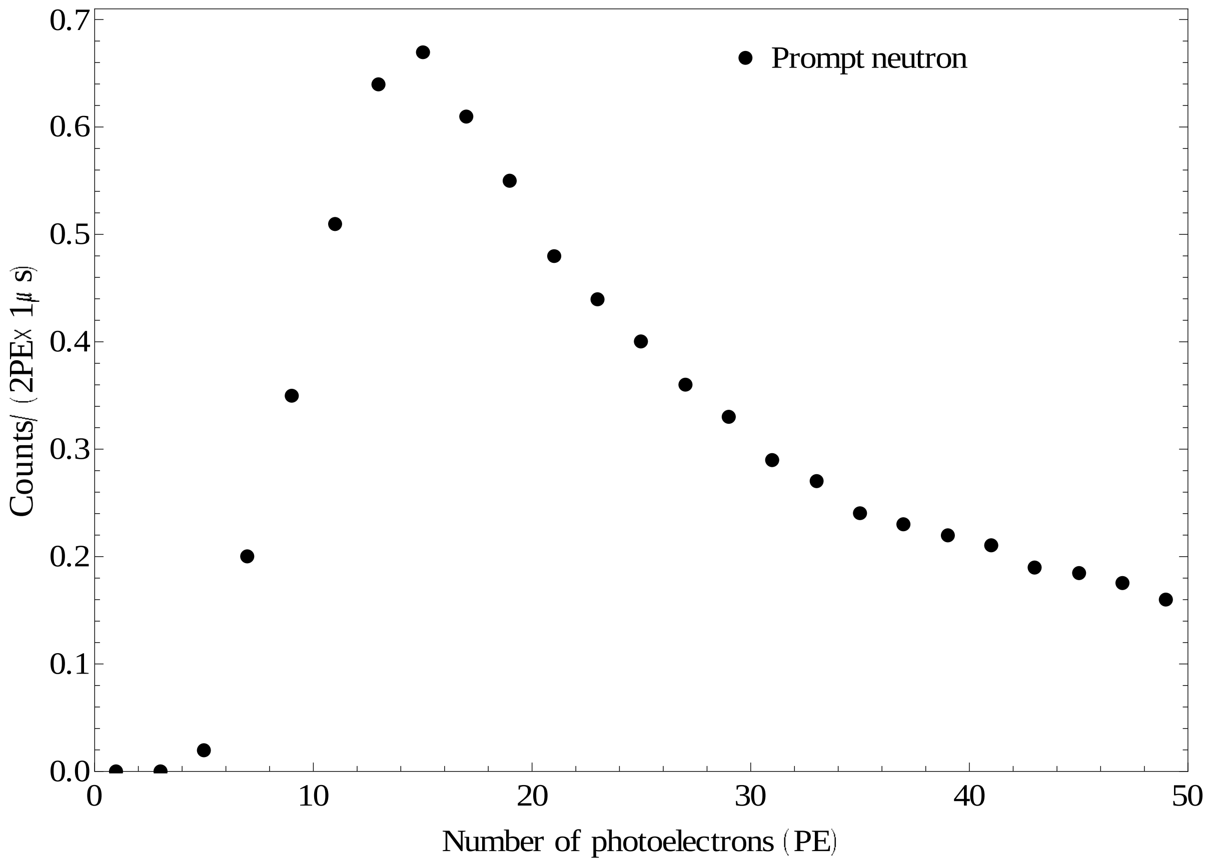

Parity Violation in Electron Scattering from PREX

PRL **108,** 112502 (2012) PHYSICAL REVIEW LETTERS week ending 16 MARCH 2012

Measurement of the Neutron Radius of ^{208}Pb through Parity Violation in Electron Scattering

[34]University of New Hampshire, Durham, New Hampshire 03824, USA
[35]University of Science and Technology of China, Hefei, Anhui 230026, People's Republic of China
[36]University of Virginia, Charlottesville, Virginia 22903, USA
[37]Virginia Polytechnic Institute and State University, Blacksburg, Virginia 24061, USA
[38]Yerevan Physics Institute, Yerevan, Armenia

(Received 12 January 2012; published 15 March 2012)

We report the first measurement of the parity-violating asymmetry A_{PV} in the elastic scattering of polarized electrons from ^{208}Pb. A_{PV} is sensitive to the radius of the neutron distribution (R_n). The result $A_{\mathrm{PV}} = 0.656 \pm 0.060(\mathrm{stat}) \pm 0.014(\mathrm{syst})$ ppm corresponds to a difference between the radii of the neutron and proton distributions $\boxed{R_n - R_p = 0.33^{+0.16}_{-0.18}\ \mathrm{fm}}$ and provides the first electroweak observation of the neutron skin which is expected in a heavy, neutron-rich nucleus.

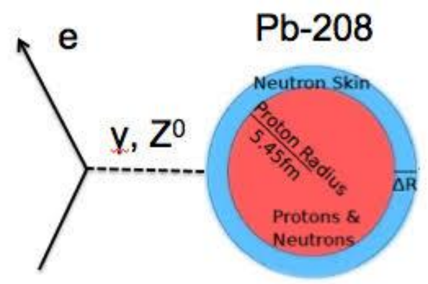

By comparing **the cross sections for left- and right-handed electrons scattered from various unpolarized nuclear targets**, the small parity-violating asymmetry can be measured

$$A_{\mathrm{PV}} = \frac{\sigma_R - \sigma_L}{\sigma_R + \sigma_L} \approx \frac{G_F Q^2}{4\pi\alpha\sqrt{2}} \frac{F_W(Q^2)}{F_{\mathrm{ch}}(Q^2)},$$

First model independent measurement of the lead neutron radius using Parity violation in electron scattering

$$\Delta R_{np}^{Pb} = 0.33^{+0.16}_{-0.18}\ \mathrm{fm}$$

Fattoyev et al. Phys. Rev. Lett. **120**, 172702

“Neutron skins and neutron stars in the multi-messenger era” ,

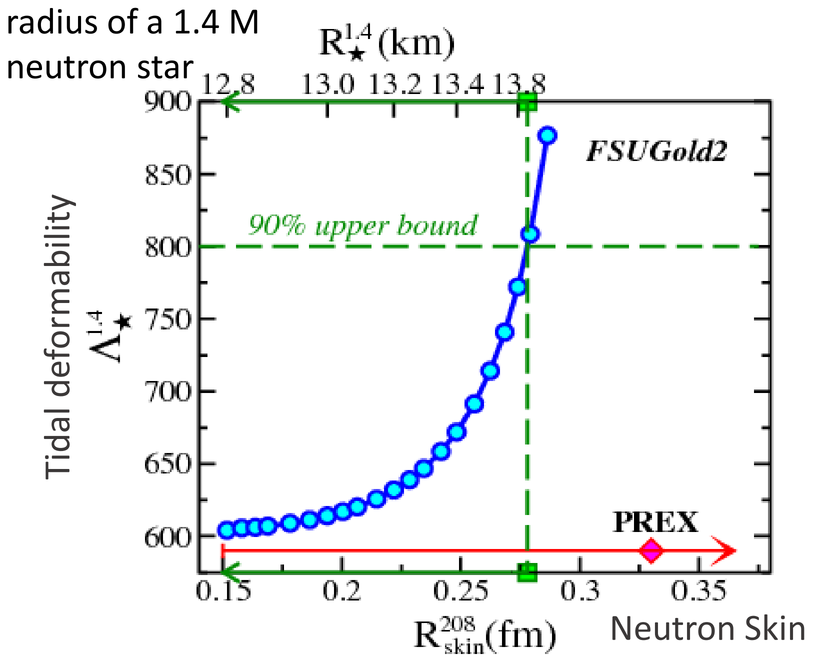

They use the FSUGold2 nuclear model to predict the tidal polarizability Λ of a 1.4 solar mass neutron star as a function of both the lead neutron skin and the radius of a 1.4 M neutron star. The 90% confidence limit on Λ 1.4 ≤800 extracted from the GW signal translates into a corresponding upper limit on the radius of a 1.40 M neutron star of R1.4 ≤13.9 km. Also shown in the figure is the central value of neutron skin as measured by the PREX collaboration. Adopting the Λ 1.4 ≤ 800 limit excludes the neutron skin>0.28 fm region.

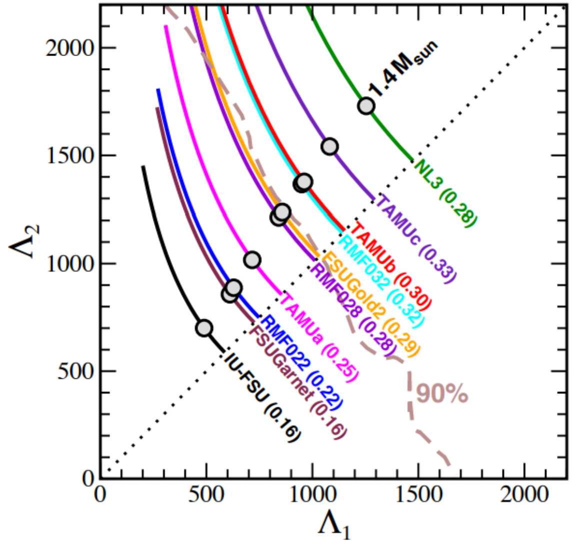

FIG. 2: (Color online). Tidal polarizabilities Λ_1 and Λ_2 associated with the high-mass M_1 and low-mass M_2 components of the binary predicted by a set of ten distinct RMF models.

However, if the large value of the neutron skin is confirmed by PREX-II, then an intriguing scenario may develop. A thick neutron skin would suggest that the EOS at the typical densities found in atomic nuclei is stiff, while the small neutron-star radii inferred from the BNS merger implies that the EOS at higher densities is soft.

The evolution from stiff to soft may be indicative of a phase transition in the interior of neutron stars.

GW170817: Measurements of neutron star radii and equation of state The LIGO Scientific Collaboration and The Virgo Collaboration, arXiv:1805.11581v1

Marginalized posterior for the tidal deformabilities of the two binary components of GW170817. The green shading shows the posterior obtained using the Λa (Λs, q) EOS-insensitive relation to impose a common EOS for the two bodies, while the green, blue, and orange lines denote 50% (dashed) and 90% (solid) credible levels for the posteriors obtained using EOS insensitive relations, a parameterized EOS without a maximum mass requirement, and independent EOSs, respectively. The grey shading corresponds to the unphysical region Λ2 < Λ1 while the seven black scatter regions give the tidal parameters predicted by characteristic EOS models for this event

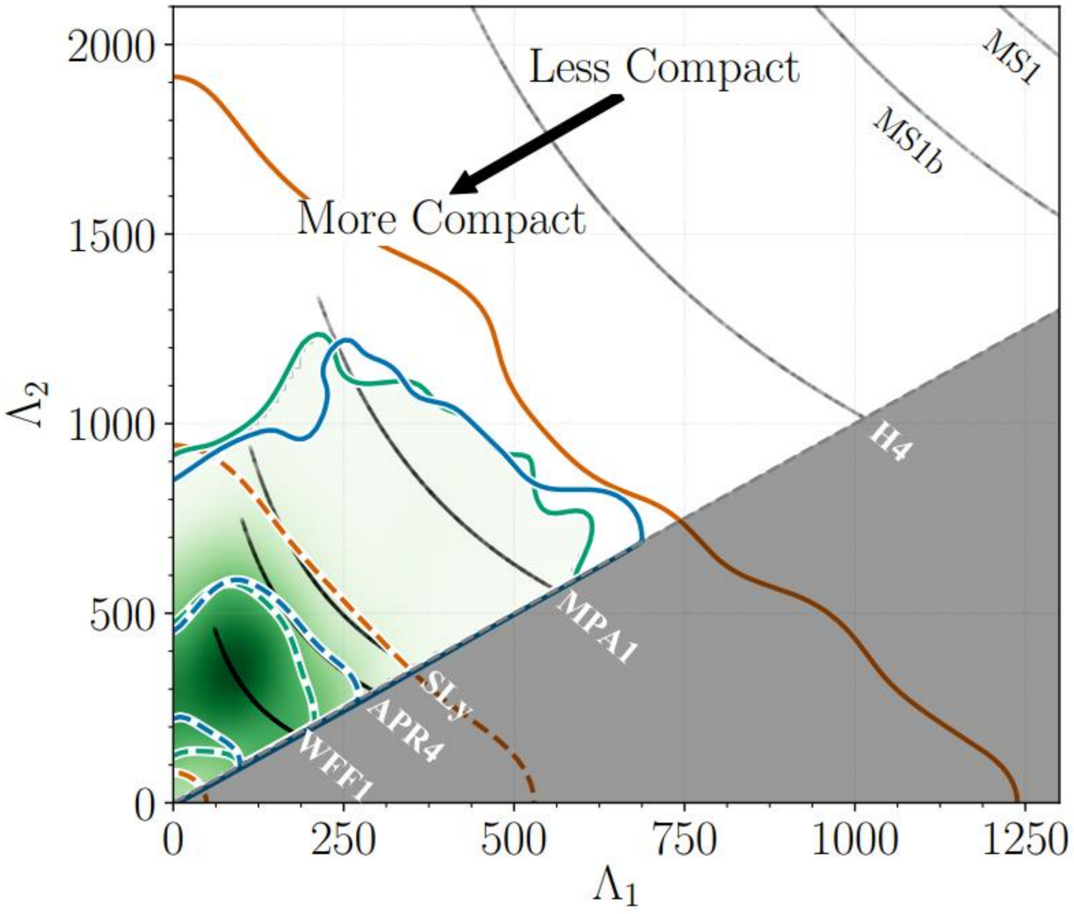

Neutron skin and implications

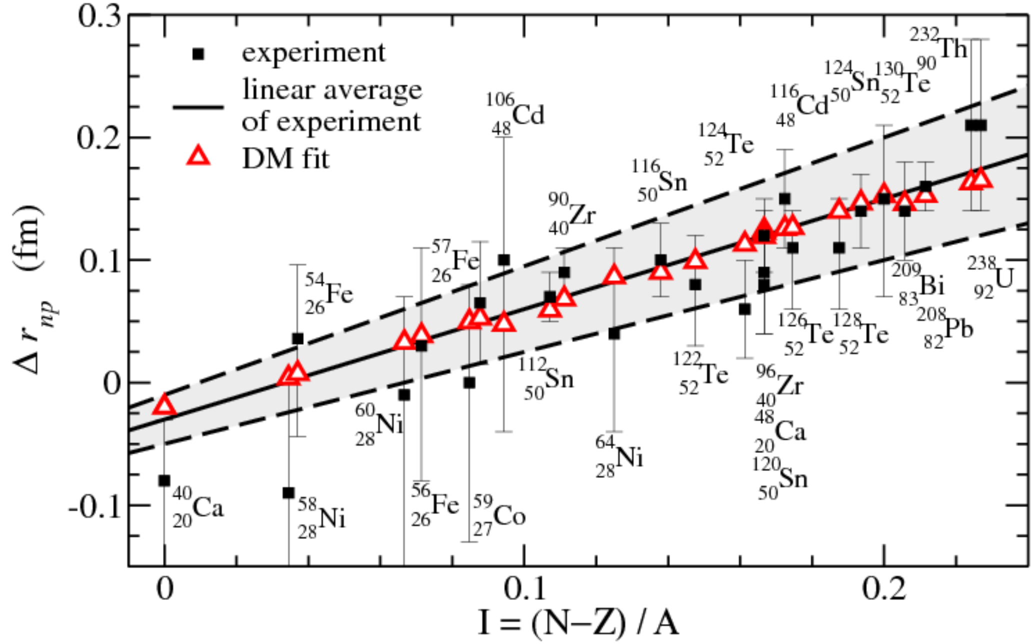

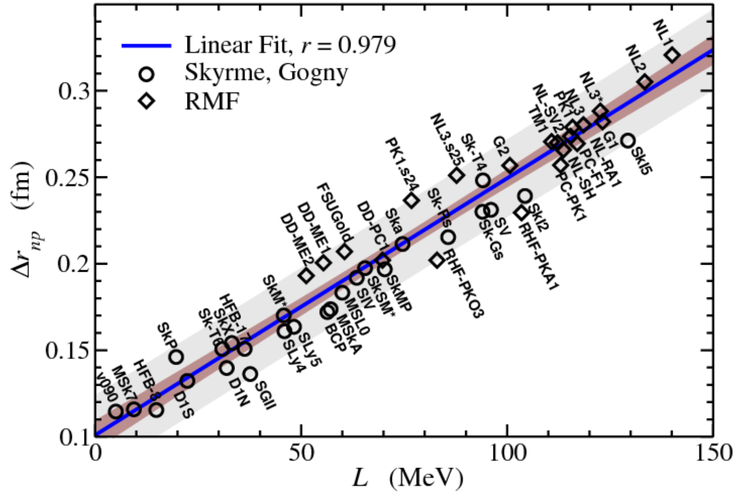

The **neutron skin is correlated with several nuclear quantities**, e.g. with the slope of bulk symmetry energy

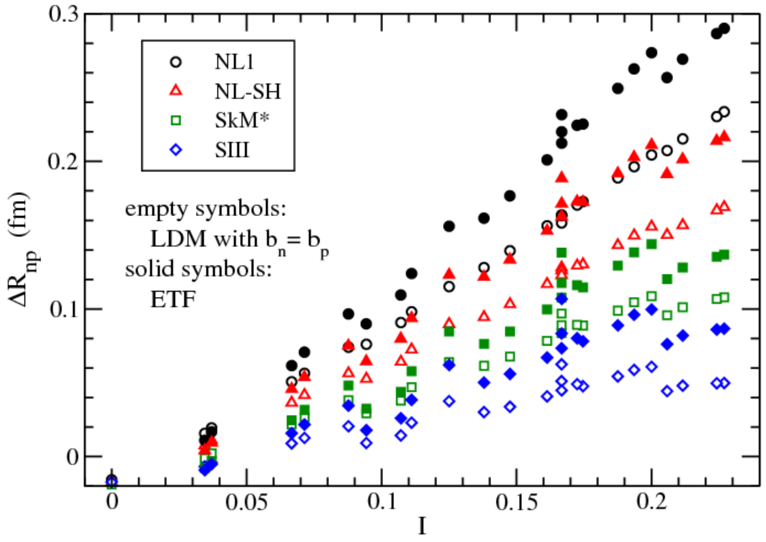

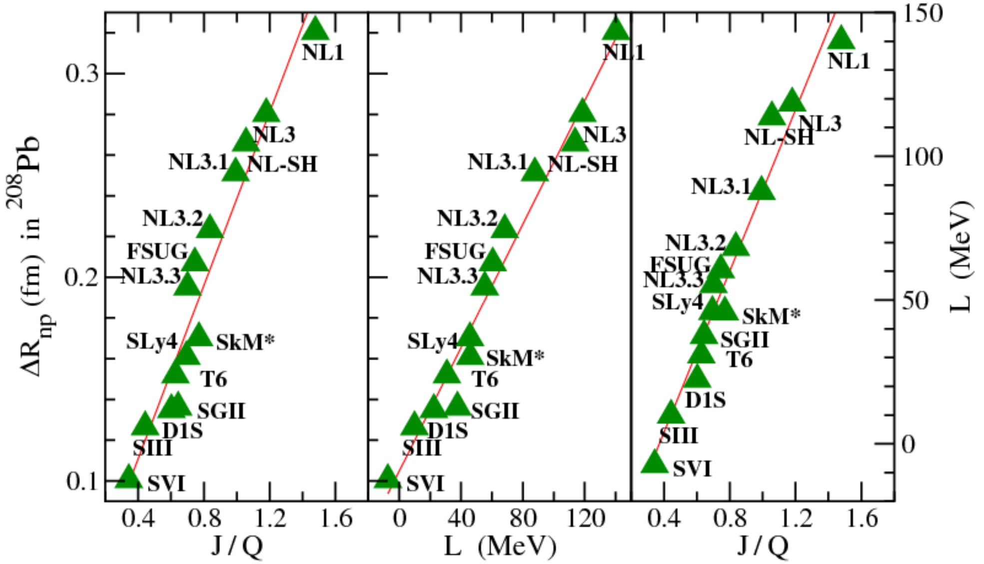

Viñas, X. *et al.* Eur. Phys. J. A50 (2014) 27

CEnNS in DM experiments

Neutrino flux and maximum recoil energy

ν	E_ν^{max} (MeV)	E_r^{max}(keV) Argon	E_r^{max}(keV) Xenon
pp	0.42	$9.6 \cdot 10^{-3}$	$2.9 \cdot 10^{-3}$
^{7}Be	0.86	0.041	0.0124
pep	1.40	0.119	0.0367
^{15}O	1.73	0.161	0.0491
^{8}B	16.4	14.6	4.5
hep	18.8	18.9	5.8
DSNB	82.5	363.3	111.3
Atm.	944	$45 \cdot 10^3$	$14 \cdot 10^3$

$$E_r^{max} = \frac{2 m_N E_\nu^2}{(m_N + E_\nu)^2} \xrightarrow{m_N \gg E_\nu} \frac{2E_\nu^2}{m_N + 2E_\nu}$$

SOLAR

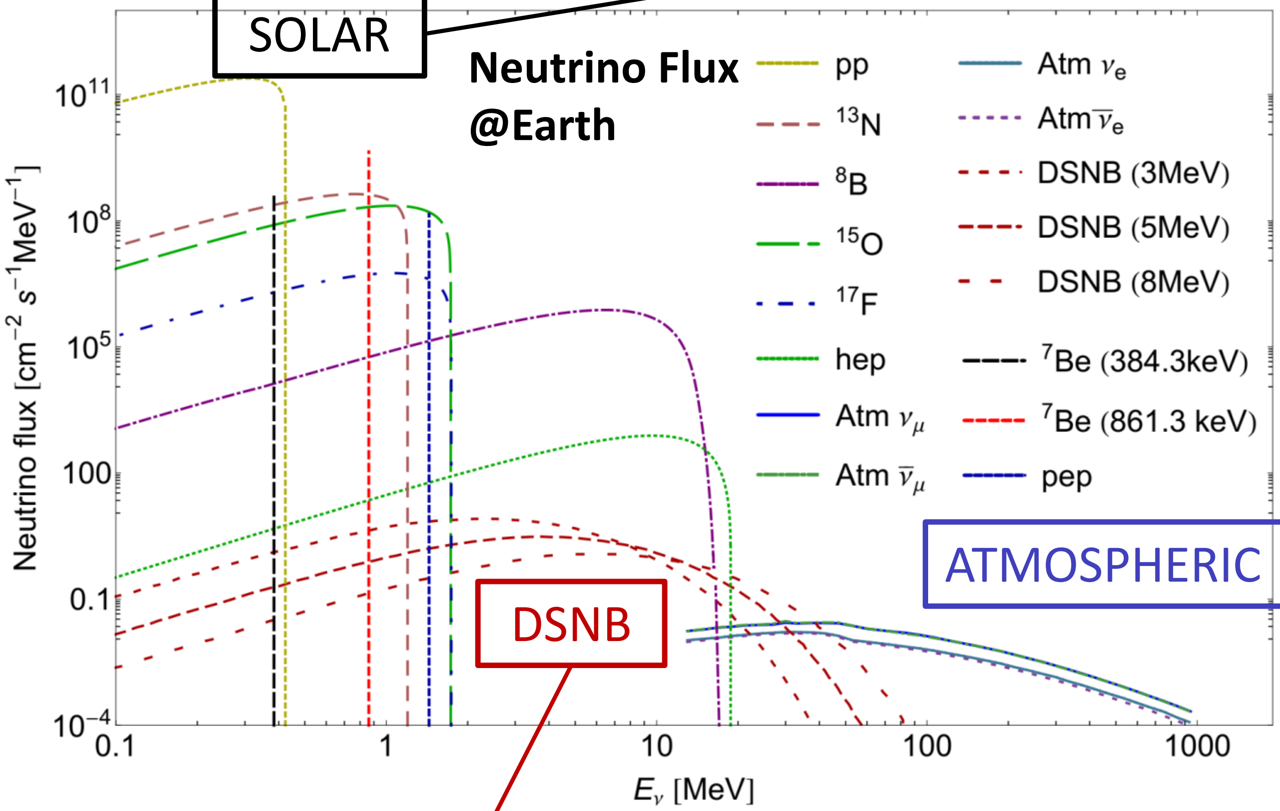

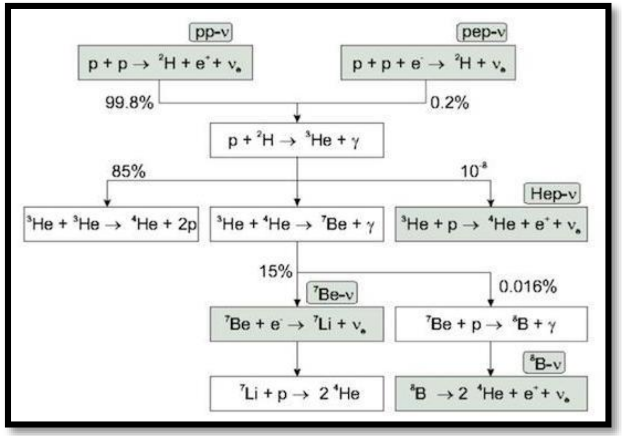

ATMOSPHERIC

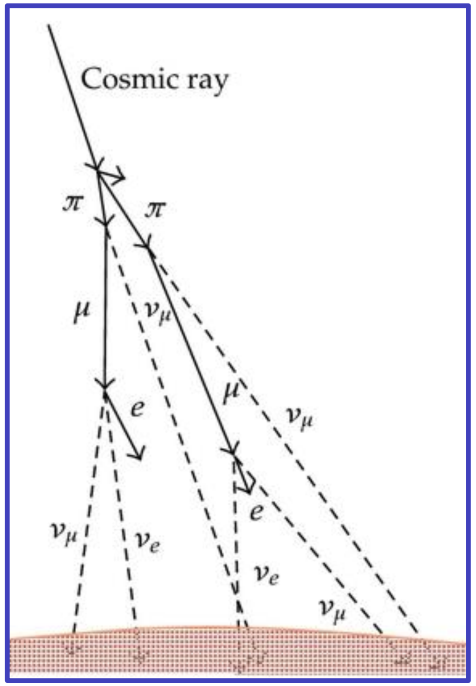

DSNB

$$\frac{d\phi(E)}{dE} = \frac{c}{H_0} \int_0 dz \frac{R_{CCSN}(z)}{\sqrt{\Omega_\Lambda + \Omega_m (1+z)^3}} \frac{dN(E')}{dE'}$$

Spectrum of a single SN emission. Fermi-Dirac spectrum for the redshifted energy E'.

$R_{CCNz}(z)$ is the rate of core-collapse SN for comoving volume as a function of the redshift z

CEnNS event rate for argon

$$\frac{d\sigma}{dE_r} = \frac{G_F^2}{4\pi} Q_W^2 m_N \left(1 - \frac{m_N E_r}{2E_\nu^2}\right) |F(E_r)|^2$$

$$\frac{dR_\nu(E_r)}{dE_r} = \eta \times \int_{E_{\nu min}} \frac{dN}{dE_\nu} \times \frac{d\sigma(E_\nu, E_r)}{dE_r} dE_\nu$$

Neutrino fluxes @Earth

$$E_\nu^{min} = \sqrt{\frac{m_N E_r}{2}} \text{ (in the limit } m_N \gg E_\nu)$$

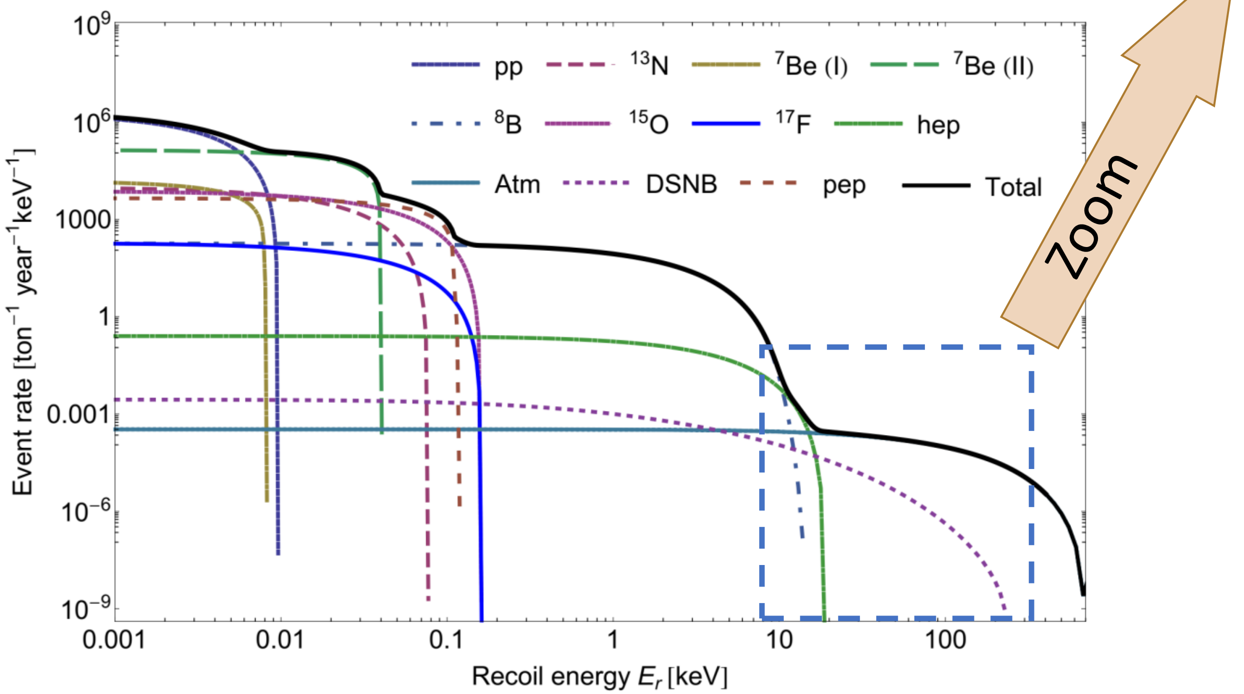

Region of interest $1 \text{ keV} \lesssim E_r \lesssim 200 \text{ keV}$

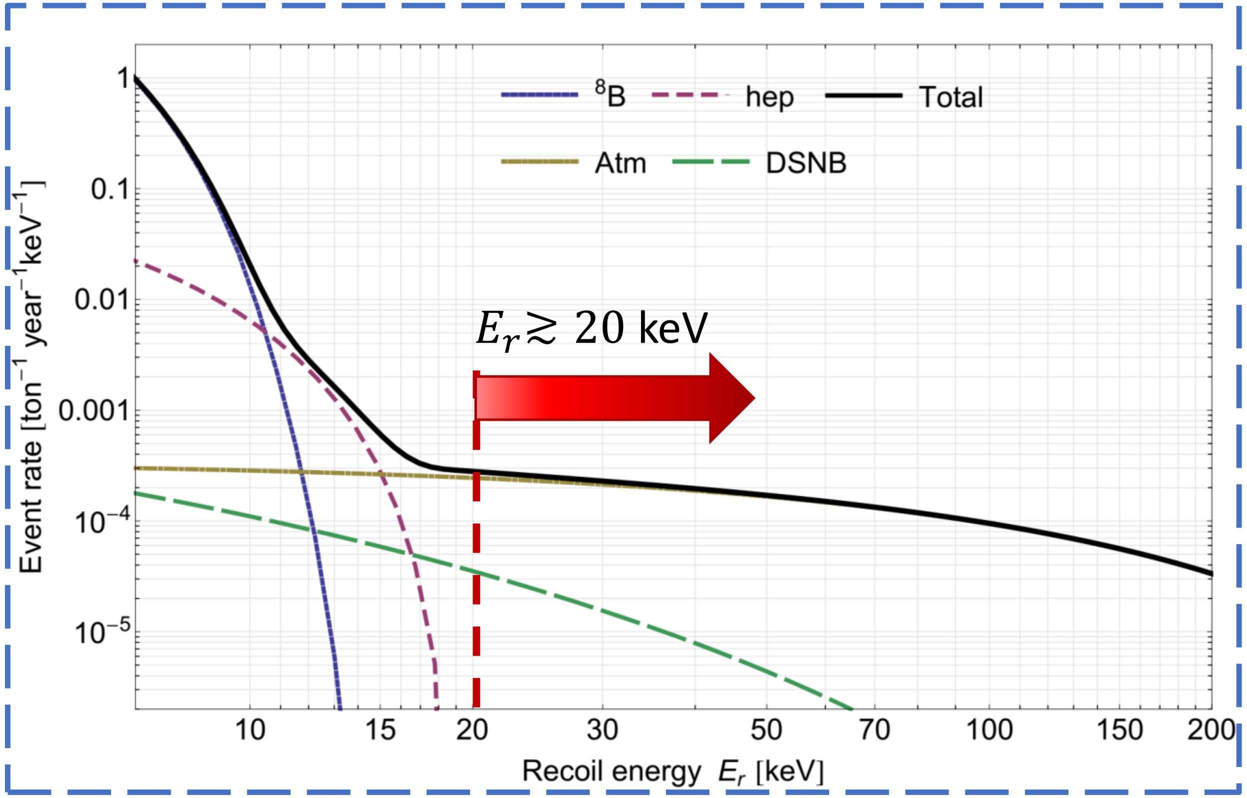

Atmospheric neutrinos are the dominant component!

Similarities between neutrino and WIMP spectrum

A WIMP signal could almost perfectly be mimicked by solar neutrino backgrounds

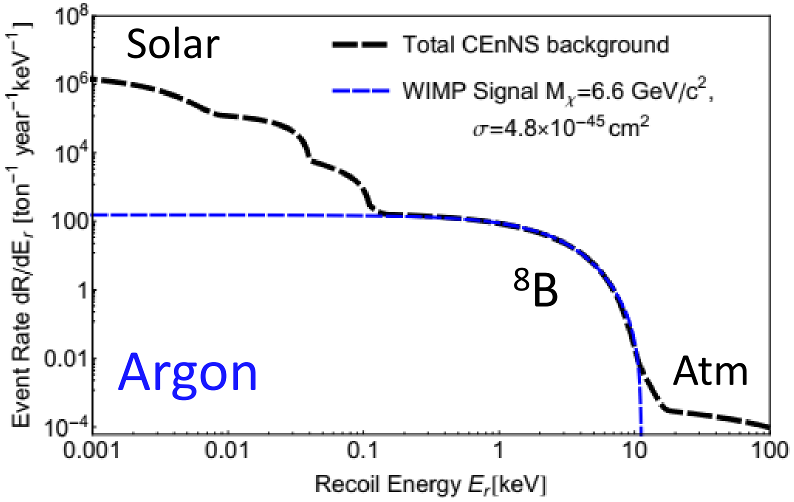

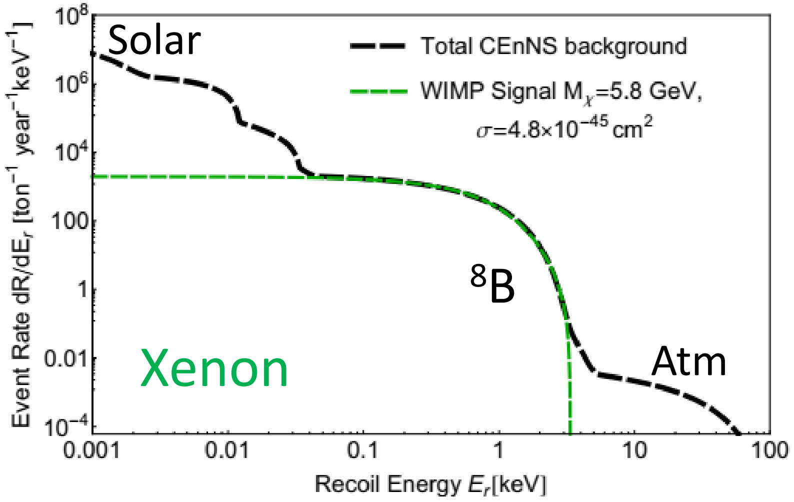

Same number of WIMP and background neutrino events but **different shape**!

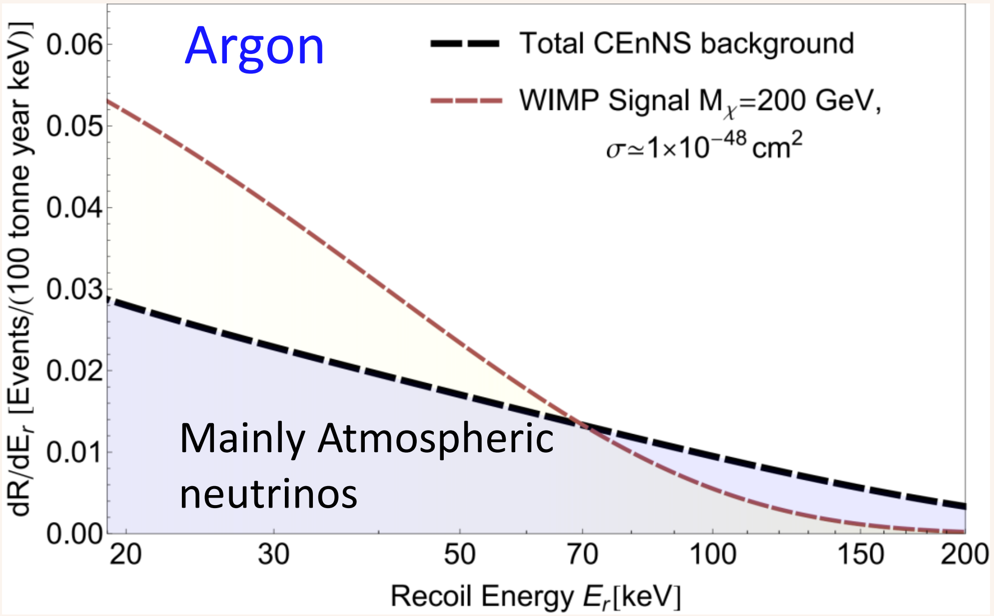

A likelihood analysis which make use of the shape information *would help in disentangling WIMP from atmospheric neutrinos*!

The “neutrino floor”

J. Billard and E. Figueroa-Feliciano (MIT)
L. Strigari (Stanford University)
PHYSICAL REVIEW **D** 89, 023524 (2015)

The “neutrino floor”

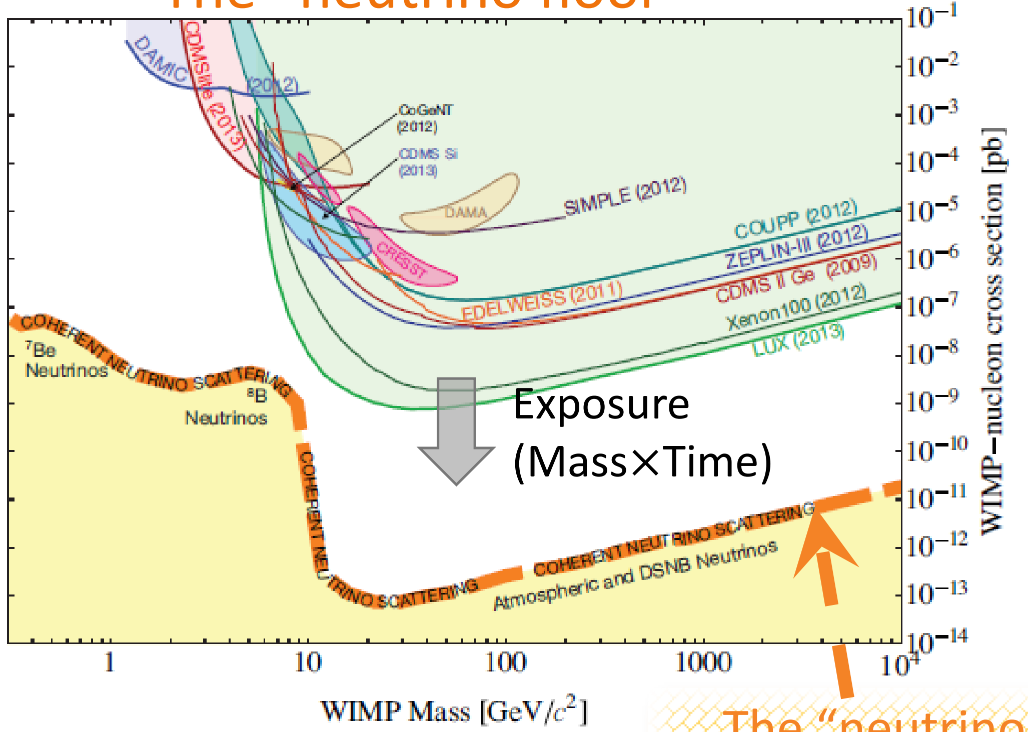

Isoevents neutrino curves

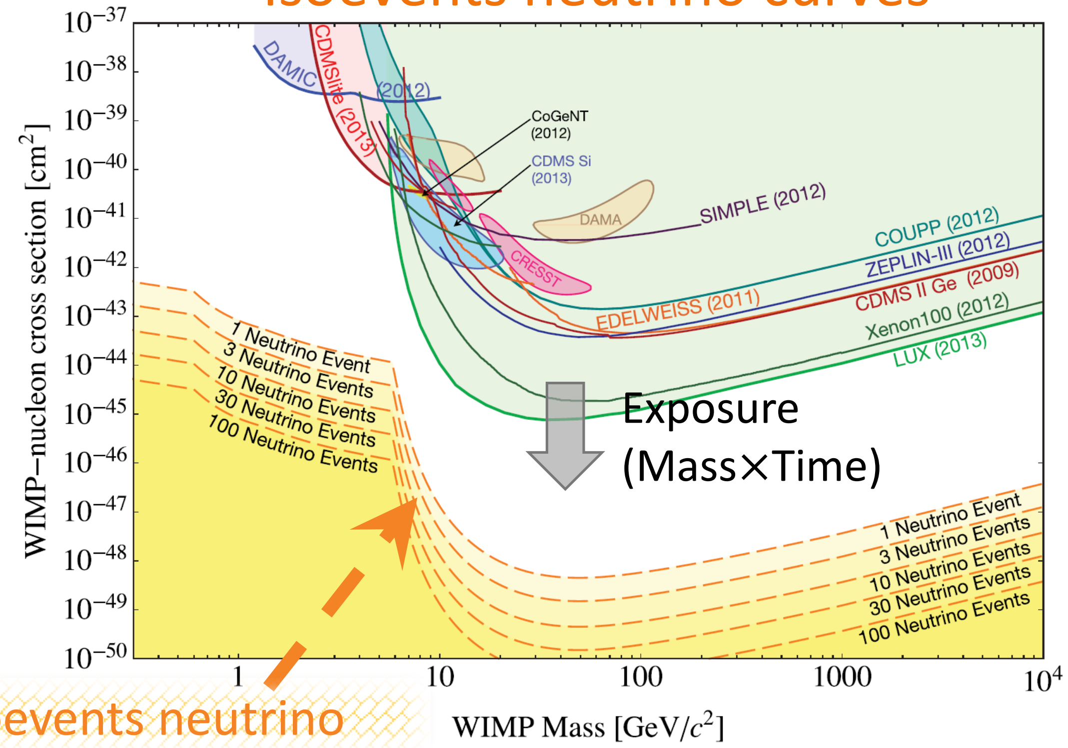

The “neutrino floor”

Isoevents neutrino curves

This limit can be shown to be the ultimate discovery limit for all direct Dark Matter experiments!

Main Assumptions:

- Xenon as a target and so it is not directly comparable with exclusion limits obtained from differet targets esperiment
- It assumes two particular **energy thresholds** [3 eV and 4 keV] and predicts **500 neutrino events** from coherent neutrino scattering on nuclei -> strong limit for DM discovery!

Best WIMP sensitivity in the presence of CEnNS (neutrino floor)

1000 background-free exclusion limits, isovalues of WIMP events (2.3 at 90% C.L.), as a function of the WIMP mass, with varying thresholds (E_{th}) from **0.001 to 200 keV** and adjusted each curve's exposure (MT) such that each experiment expects a neutrino background of one event.

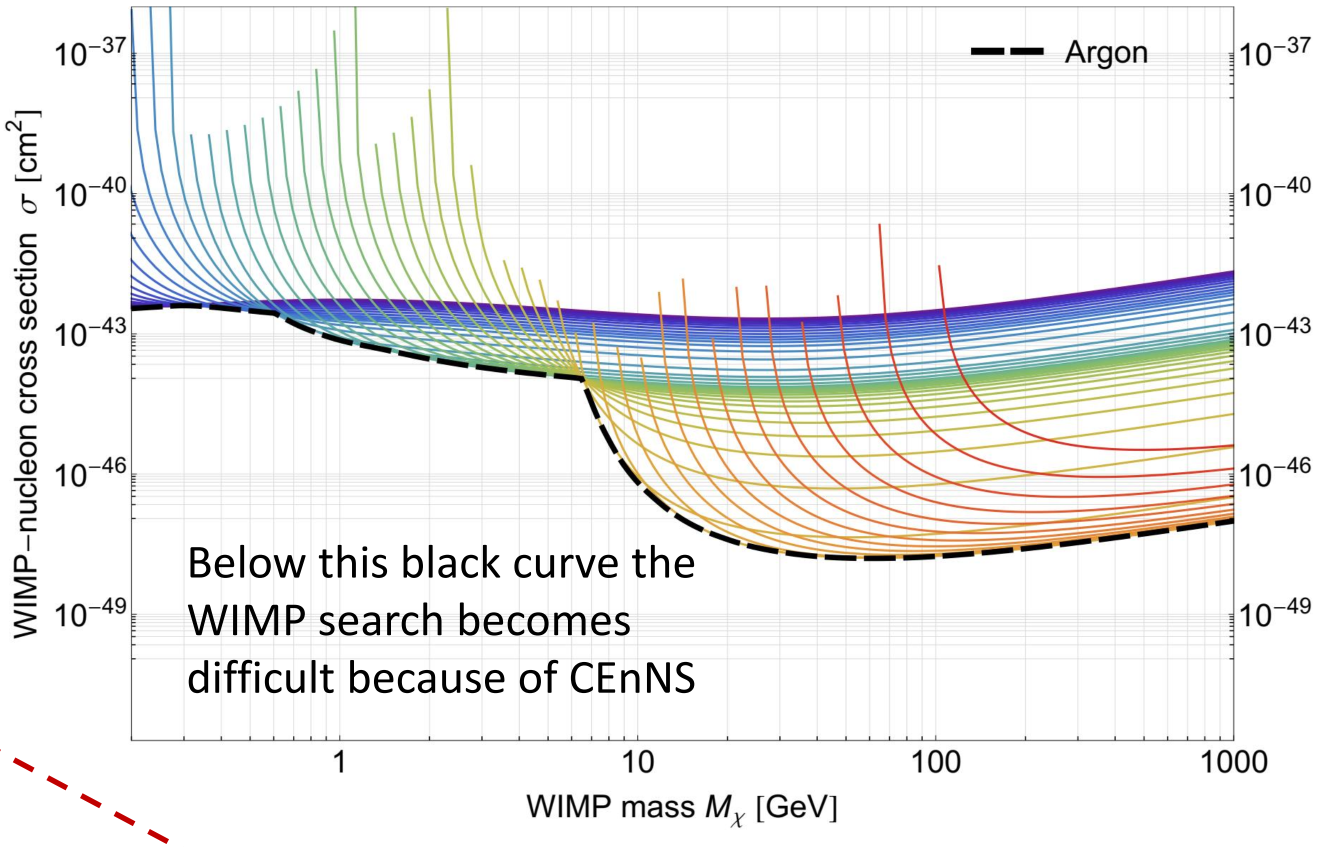

$$\hat{\sigma}_{90\%}(E_{th}, M_\chi) = \frac{2.3}{\boxed{(MT)_{1\,neutr}} \times \boxed{\int_{E_{th}}^{E_{up}} \frac{dR_\chi}{dE_r} dE_r}}$$

Coherent elastic neutrino nucleus background

$$\frac{dR_\nu(E_r)}{dE_r} = \eta \times \int_{E_{\nu_{min}}} \frac{dN}{dE_\nu} \times \frac{d\sigma^{CNS}(E_\nu, E_r)}{dE_r} dE_\nu$$

$$(MT)_{1\,neutr} = \frac{1\ \nu\ events}{\int_{E_{th}}^{E_{up}} \frac{dR_\nu}{dE_r} dE_r\ \ [\nu\ events\ ton^{-1} year^{-1}]}$$

WIMP-nucleus recoil spectrum

$$\frac{dR_\chi}{dE_r} = \frac{\sigma_{w-n}}{2M_w\,\mu_n^2} A^2 F^2(E_r)\,\rho_0 \int \frac{f_1(v)}{v} dv$$

Comparison between argon and xenon isoevents curve

Billard et al. Phys. Rev. D 89, 023524 (2014)

M. Cadeddu and E. Picciau, «Impact of neutrino background prediction for next generation dark matter detectors", JPCS 956 n.1, 012014 (2018)

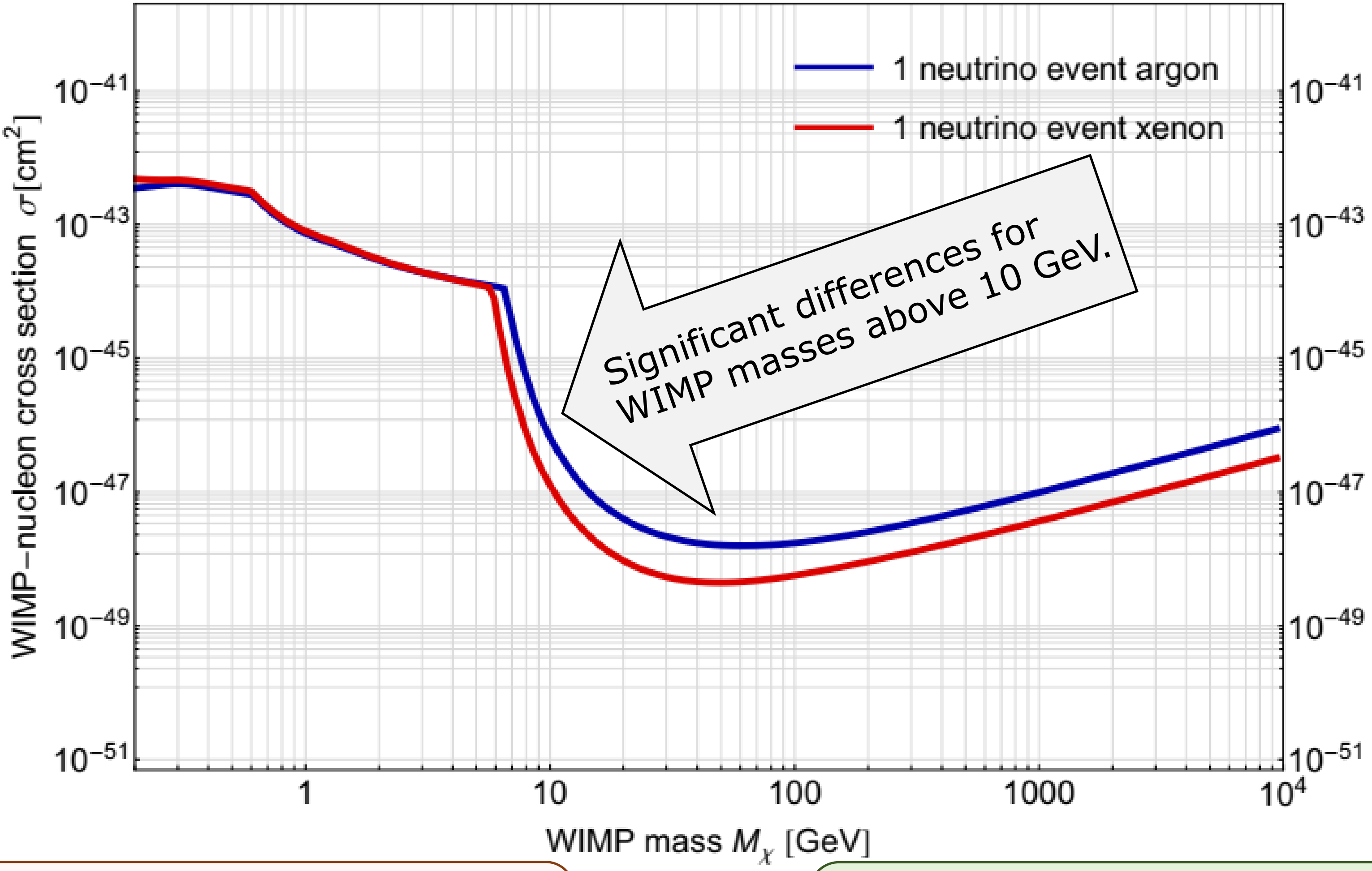

Xenon

$\sigma_{\chi-n}(M_\chi = 100\ \text{GeV}) = 5.6 \cdot 10^{-49}\ \text{cm}^2$

Argon

$\sigma_{\chi-n}(M_\chi = 100\ \text{GeV}) = 1.7 \cdot 10^{-48}\ \text{cm}^2$